universität wien

MASTERARBEIT | MASTER'S THESIS

Titel | Title

Attempts for the Stereoselective Synthesis of Pantaphos and its Analogues

verfasst von | submitted by

Naomi Müller BSc BSc

angestrebter akademischer Grad | in partial fulfilment of the requirements for the degree of

Master of Science (MSc)

Wien | Vienna, 2026

Studienkennzahl lt. Studienblatt | Degree programme code as it appears on the student record sheet:	UA 066 862
Studienrichtung lt. Studienblatt | Degree programme as it appears on the student record sheet:	Masterstudium Chemie
Betreut von | Supervisor:	Dr. Katharina Pallitsch Privatdoz. Bakk. MSc

Acknowledgments

Zuerst möchte ich meiner Betreuerin den allergrößten Dank aussprechen. Vielen Dank für die Möglichkeit meine Arbeit in deiner Gruppe machen zu dürfen, für die grandiose Unterstützung sowohl im Labor als auch außerhalb davon, und die durchwegs hohe Motivation neue Ideen umzusetzen, Probleme zu lösen und allem voraus die Freude dabei nicht zu verlieren!

Ein besonderer dank gilt der gesamten Arbeitsgruppe, angefangen bei Sebi, für seine wertvolle Hilfe während der gesamten Arbeit, sowie für die absurdesten Fun Facts in den vergangenen Monaten. Des Weiteren möchte ich mich bei Flo bedanken. Es ist mir bis zum heutigen Tag ein Rätsel wie man sich mit solchen Kommunikationsschwierigkeiten so problemlos einen Abzug teilen kann. Ebenso gilt mein Dank Tina, für interessante Gespräche und ideenreiche Diskussionen in den Kaffeepausen. Auch wenn wir nur kurze Zeit zusammengearbeitet haben, gilt mein Dank ebenso Annika, die mir vor allem im Endspurt große Motivation schenkte.

Abschließend möchte ich mich von Herzen bei Lukas und meiner Familie bedanken. Auch wenn uns viele Kilometer trennen, wart ihr mir während des Studiums eine wahnsinnige Unterstützung und habt mich immer darin bestärkt, das zu tun, was mir Spaß macht!

Vielen Dank!

Zusammenfassung

Die Akkumulation, Verteilung und der Abbau von Herbiziden spielen eine entscheidende Rolle für die Umwelt. Daher sind detaillierte Kenntnisse über deren Metabolismus essenziell, um umweltfreundlichere, weniger schädliche und besser wirksame Herbizide zu entwickeln.

Phosphonate (Pns) zeichnen sich durch ihre einzigartige Kohlenstoff-Phosphor-Bindung aus und weisen hervorragende Eigenschaften für diverseste Anwendungen auf. Unter den Pn-basierten Stoffen befinden sich auch Verbindungen mit herbizider Wirkung, wie beispielsweise Glyphosat oder Phosphinothricin. Während diese bereits kommerziell erhältlich sind, werden die Eigenschaften und der mögliche Einsatz von Pantaphos noch intensiv erforscht. Diese Arbeit konzentriert sich daher auf die stereoselektive Synthese der vier möglichen Isomere von Pantaphos und deren gesättigter Analoga. Pantaphos beinhaltet neben dem Phosphor-Atom eine α-Hydroxy-Gruppe mit unbekannter Konfiguration. Geplant war eine enantioselektive Synthese, da bisher nur razemisches Pantaphos synthetisch hergestellt werden konnte. Mit diesen Enantiomeren kann die finale Strukturaufklärung von Pantaphos erfolgen und die herbiziden Eigenschaften der Enantiomere können separat bestimmt werden. Die Rolle der Doppelbindung für die Wirksamkeit soll durch die Synthese der beiden gesättigten Analoga von Pantaphos untersucht werden.

Für die Lösung dieser Syntheseprobleme wurden verschiedene Routen getestet. Die erste Syntheseroute basiert auf einer Fráter Seebach Alkylierung, gefolgt von einer *O*-Dealkylierung und einer anschließenden Schützung der Hydroxy-Gruppe, um das Zwischenprodukt **35** zu erhalten. Aufgrund geringer Ausbeuten in den ersten Schritten, wurden alternative Reaktionsbedingungen und Elektrophile getestet. Leider war enantiomerenreines Pantaphos durch diese Methode nicht zugänglich. Daher wurden Versuche unternommen um das Grundgerüst von Pantaphos, durch eine Reaktion zur Bildung einer C-P Bindung zwischen einem Phosphit und Anhydriden wie Bernsteinsäure- oder Maleinsäureanhydrid, aufzubauen. Das Grundgerüst konnte auf diese Weise dargestellt werden, wenn auch unter Verlust einer Schutzgruppe. Die Route lieferte vielversprechende erste Ergebnisse und wird daher als Grundlage für künftige Versuche dienen, um (*R*)- und (*S*)-Pantaphos zu synthetisieren.

Abstract

Accumulation, distribution and breakdown of herbicides play a crucial role for the environment. Therefore, a detailed knowledge about their metabolic behaviour is essential for the design of eco-friendly and less harmful herbicides, with high efficiency.

Phosphonates (Pns), characterized by a unique carbon-phosphorus bond, exhibit outstanding properties which form the basis for a variety of applications of both biogenic and synthetic Pns. Among Pn-based drugs, also herbicidal compounds, such as glyphosate or phosphinothricin can be found. While the latter are already commercialized, the properties and potential uses of pantaphos are still under investigation. Therefore, this work focuses on the stereoselective synthesis of pantaphos and its saturated analogues. This compound bears an α-hydroxy group of unknown configuration next to the phosphorus atom. Until now, only racemic pantaphos was obtained synthetically. With the enantiomers in hands, the structural elucidation of the absolute configuration of biogenic pantaphos will become possible and the herbicidal properties of the enantiomers can be evaluated separately. The role of the double bond for the activity of pantaphos is planned to be studied by synthesizing saturated analogues of the natural product.

Different synthesis routes were tested to tackle this synthetic problem. The first synthetic route relied on a Fráter Seebach alkylation with dialkyl malate as starting material, followed by *O*-dealkylation and a subsequent protection of the hydroxy group to give key intermediate **35**. Due to consistently low yields, a variety of conditions and electrophiles were tested as alternative. Unfortunately, enantiopure pantaphos could not be accessed by this method. Therefore, efforts to access the core structure of pantaphos by forming a C-P bond between a phosphite and anhydrides like succinic or malic anhydride were undertaken. Pleasantly, the intended core could be obtained by this approach, albeit with simultaneous loss of one protecting group. The latter route showed promising first results and will thus form the basis for future attempts to access (*R*)- and (*S*)-pantaphos.

Table of Content

1. Introduction

1.1. Phosphorus and Organophosphorus Compounds

Life on earth highly relies on phosphorus compounds. They are known to occur in various oxidation states from -III to +V. However, naturally the greatest relevance emanates from compounds with oxidation state +V.[1] The main classes of phosphorus containing compounds found in nature are phosphates and phosphate esters, with their typical P-O bonds. Phosphorus compounds are of high biochemical relevance, as phosphate esters not only build up the backbone of DNA and RNA, encoding the genetic code, but are also a key component of adenosine triphosphate (ATP), the universal energy supplier in living cells and a key component for cellular signal transduction.[2] Phosphonates are another class of phosphorus-containing natural products, with a unique carbon-phosphorus (C-P) bond (Figure 1).

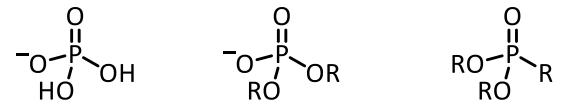

Figure 1 – Structural comparison of phosphate, phosphate esters and phosphonates.

Phosphonates are nearly isosteric to phosphate esters, but can resist harsher chemical conditions, like strong bases or acids. Their stability even protects them from enzymatic degradation by phosphatases. Therefore, phosphonates are highly investigated as drugs in pharmaceutical and agricultural industry and the interest in fundamental questions about their biochemistry and metabolism by microorganisms is constantly rising.[3]

1.2. Phosphonates as Drugs

Phosphonic acids and phosphonates have a broad medical application spectrum due to their outstanding chemical properties in combination with their structural similarities to other important compound classes, often making them good mechanism-based enzyme inhibitors. In many established drugs, non-hydrolysable phosphonates are used to inhibit phosphate metabolizing enzymes, but also other inhibition modes are known. Established phosphonate based drugs are both of natural (fosfomycin or phosphinothricin, e.g.) and synthetic (foscarnet or zoledronate, e.g.) origin (Figure 2).[4]

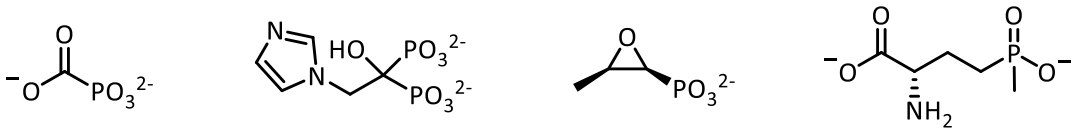

Foscarnet, **1** Zoledronate, **2** Fosfomycin, **3** Phosphinothricin, **4**

Figure 2 – Commercialized phosphonic- and phosphinic acids of pharmaceutical and agricultural relevance.[5]

1.2.1. Foscarnet (**1**)

Phosphonoformate, also known as Foscarnet (**1**), is applied for the treatment of herpes simplex. Foscarnet blocks the pyrophosphate receptor site of the viral DNA-polymerase and reverse transcriptase during replication by mimicking pyrophosphate. DNA chain elongation is inhibited, and pyrophosphate exchange is prevented. Foscarnet is a non-competitive inhibitor of deoxyribonucleoside triphosphate (DNP) and an uncompetitive inhibitor of the activated DNA primer.[6] In contrast to many other virostatics, no intra-cellular phosphorylation is required for activity.[7]

1.2.2. Zoledronate (**2**)

Bisphosphonates are primarily used in the treatment of various bone-related diseases. They promote bone mineral density, enhance bone remodeling and suppress bone turnover, to name but a few advantages. Zoledronate (**2**) is a nitrogen containing bisphosphonate acting as pyrophosphate analogue, thereby targeting the mevalonate pathway (Figure 3).[3]

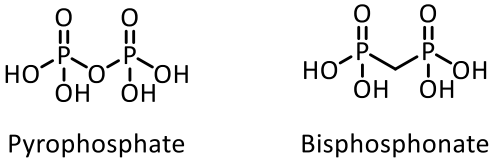

Figure 3 – Structural comparison of pyrophosphate (left) and the bisphosphonate motif (right).

The mevalonate pathway is essential for the synthesis of cholesterol and isoprenoids, which is important for maintaining the integrity of cell membranes, producing steroids and the regulation of cellular respiration along with the control of cell proliferation, cell death and tumor progression.[8] Zoledronate inhibits farnesyl pyrophosphate synthase (FPPS) and geranylgeranyl pyrophosphate synthase (GGPPS). It prevents the synthesis of geranyl pyrophosphate (**GPP**), farnesyl pyrophosphate (**FPP**) and geranylgeranyl pyrophosphate (**GGPP**) from isopentenyl pyrophosphate (**IPP**) and dimethylallyl pyrophosphate (**DMPP**) (Scheme 1).[9]

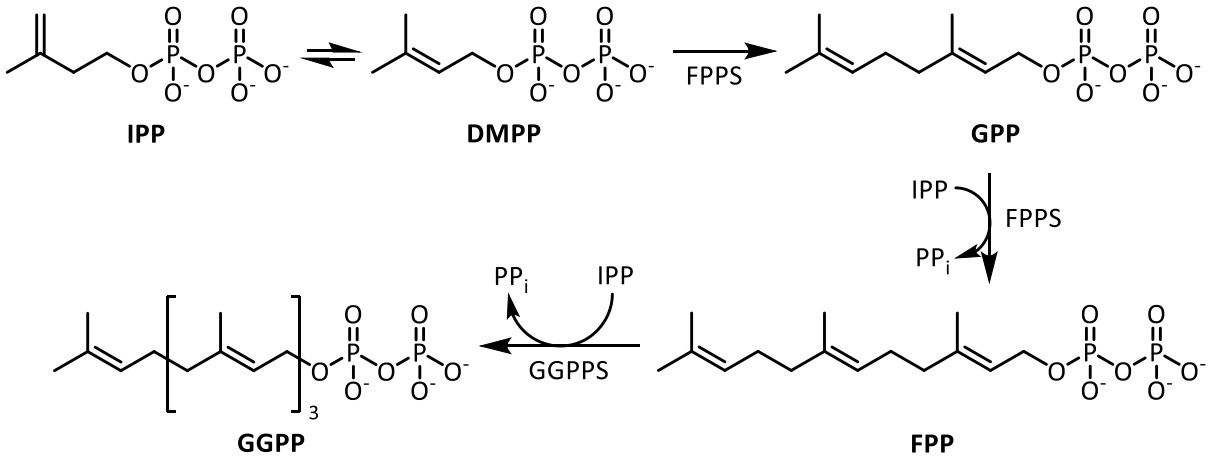

Scheme 1 – Natural mode of action of FPPS and GGPPS starting from IPP and DMPP; PP_i = pyrophosphate.

1.2.3. Fosfomycin (**3**)

Fosfomycin (**3**) is a naturally occurring broad spectrum antibiotic and was originally discovered in the fermentation broth of *Streptomyces fradiae* cultures.[10] First, it was used for the treatment of urinary tract infections but more recently it is applied against many important pathogens such as *Streptococcus pneumoniae*, *S. aureus*, *E. coli* or varied *Enterobacter* species.[10] No cross-resistance to other antibiotics is known due to its structure and unique mode of action. Fosfomycin targets the enzyme UDP-*N*-acetylglucosamine-

enolpyruvyltransferase (MurA), by acting as phosphoenolpyruvate (PEP, **5**) analogue. MurA is important in peptidoglycan synthesis for catalyzing the reaction between UDP-*N*-acetylglucosamine (**UNAG**) and PEP to give UDP-enolpyruvyl-*N*-acetylglucosamine (**UEPNAG**) (Scheme 2, Top).[11]

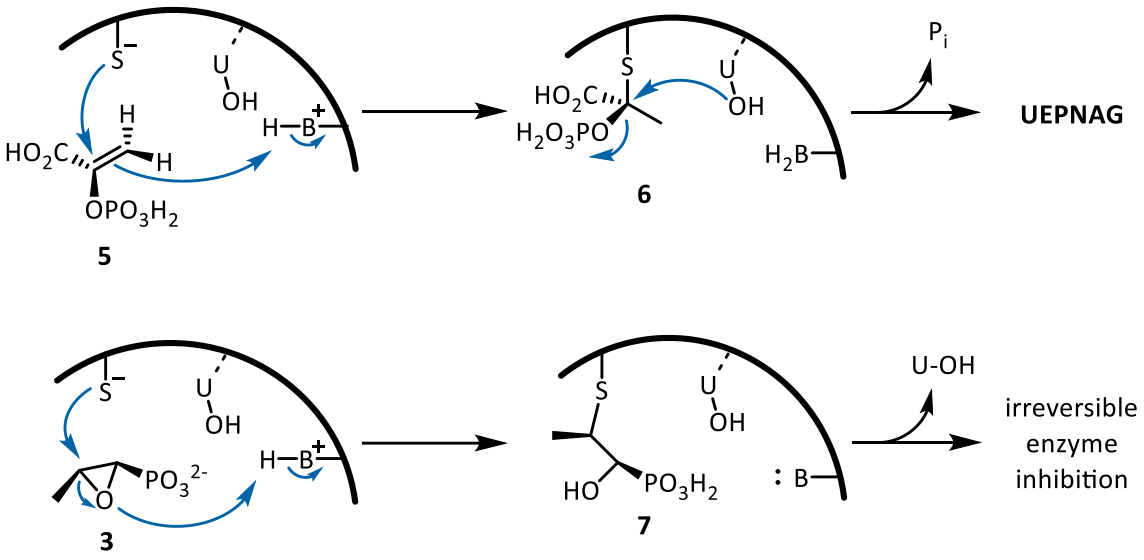

Scheme 2 – Top: Enzymatic mechanism of MurA reacting PEP and UNAG to give UEPNAG, Bottom: Irreversible enzyme inhibition mechanism by fosfomycin; B = base, U = UNAG, P_i = inorganic phosphate.[12]

This results in irreversible enzyme inhibition after epoxide opening (structure **7**, Scheme 2, Bottom).[11] Interestingly, the phosphonic acid moiety is not responsible for the bioactivity of this compound.

1.2.4. Phosphinothricin (**4**)

In contrast to the latter three compounds, the phosphinate (bearing two C-P bonds) phosphinothricin (**4**) is used in agriculture. It is the active ingredient of numerous herbicides and a structural analogue of the amino acid glutamate. Phosphinothricin irreversibly inhibits glutamine synthase after phosphorylation leading to structure **11** (Scheme 3). This ATP-dependent enzyme normally catalyses the conversion of glutamate (**8**) to glutamine (**10**) which is a necessity for ammonia assimilation in plants.[13] The inhibition leads to an increase in ammonia concentration and consequently to death of the plants.[14,15]

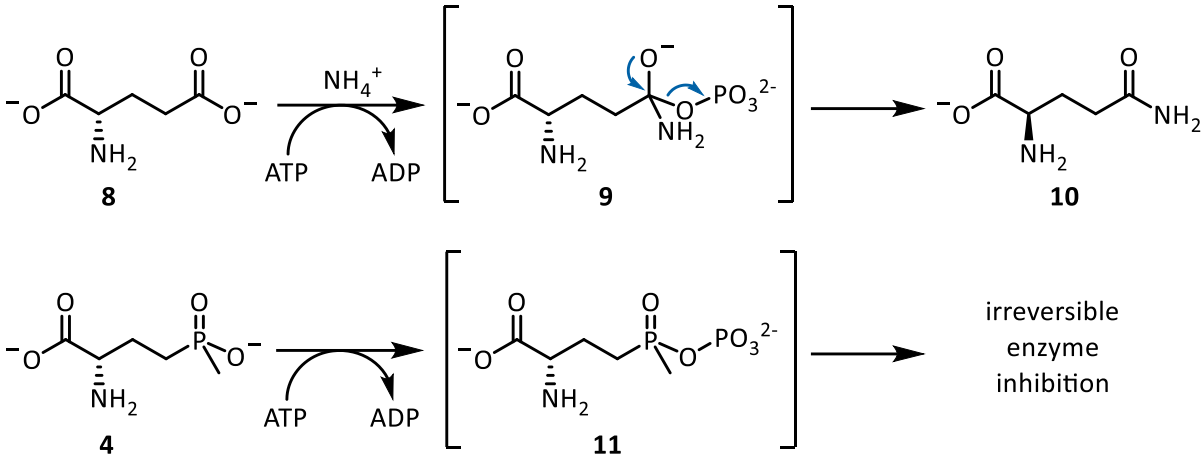

Scheme 3 – Top: natural reaction of glutamine synthase; Bottom: mode of action of phosphinothricin.[14]

1.3. Herbicides and their Environmental Effects

Herbicides like phosphinothricin are chemical compounds, designed to protect seeds and crops against adverse insects, weeds or diseases. As hand weeding is time consuming, costly and needs available labourers, there has been a drastic increase in interest in herbicides, due to the overall economic growth. Approximately 47.5 % of the pesticides utilised in 2022 correspond to herbicides, which control weeds and contribute to elevated crop yields.[16–18] As a result of increasing resistance to established herbicides (caused by their excessive use), genetically modified crops were invented. There, existing traits are improved or new traits are implemented. Genetically modified plants can be characterized, for example, by higher herbicide tolerance, various disease- and insect resistances or abiotic stress tolerance. Especially, when weeds and crops share a strong similarity, the invention of herbicide tolerant traits enables a more selective way to exterminate weeds.[19]

Despite the advantages of herbicides, often only a small amount of the applied dose reaches the target organism. Depending on the composition, persistence and behaviour of the applied herbicides, their migration represents a major concern for surrounding life.[16,17] The remaining chemical compounds penetrate the soil, accumulate and undergo multiple transformations to a variety of metabolites. Such soil metabolites can get distributed *via* air, water or bottom deposits, thereby affecting other ecosystems.[17] Therefore, numerous severe side effects of established herbicides are known. The environment as well as human- and animal health gets affected through off-target effects and high environmental persistence. This emphasizes the necessity to develop herbicides with high selectivity and specificity, low toxicity alongside environmentally friendly properties, ideally at low application doses. Especially the selectivity is intricate as crops and weeds frequently share a high homology.[16] Degradation and mobility of herbicides and their respective metabolites depend strongly on the chemical properties of the herbicide itself, interactions with surrounding chemicals and other environmental conditions.[20]

Herbicides can be applied in a selective and a non-selective manner. Non-selective herbicides are used for total vegetation-removal and are commonly used prior to sowing or alternatively in cultivars which were genetically modified to resist such circumstances.[21] Selective herbicides target specific crop species and act on designated metabolic pathways. The categorisation of herbicides, developed by the HRAC (Global Herbicide Resistance Action

Committee), is dependent on both the compound's chemical properties and the mode of action. Common modes of action rely on inhibiting the biosynthesis of amino acids, fatty acids or lipids, but also photosynthesis inhibitors or carotenoid biosynthesis inhibitors, which damage chlorophyll pigments, are known.[17]

Examples of known selective herbicides are Atrazine [**12**, 6-chloro-*N*-ethyl-*N*'-(1-methylethyl)-1,3,5-triazine-2,4-diamine] and 2,4-dichlorophenoxyaceticacid (**13**, 2,4-D, Figure 4).

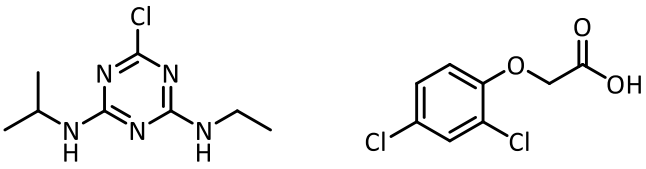

12 **13**

Figure 4 – Chemical structures of Atrazine (left) and 2,4-D (right).[17]

Atrazine targets photosynthesis, disabling photosystem II in higher plants.[22] It inhibits the light reaction by competing with plastoquinone, resulting in blockage of the electron flow to cytochromes and the formation of singlet oxygen, which is fatal for sensitive dicots. Monocots, like maize or sorghum, exhibit high activity of glutathione *S*-transferase, leading to detoxification of atrazine and the survival of the plant.[23]

2,4-D was the first introduced herbicide for broadleaf weeds. It mimics auxin, which results in uncontrolled plant growth, epinasty, growth inhibition and ultimately death of the plant.[24]

1.4. Glyphosate

Glyphosate [**14**, *N*-(phosphonomethyl) glycine, Figure 5] is worldwide the most utilised universal, non-selective herbicide.

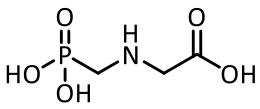

14

Figure 5 – Chemical structure of glyphosate.

The global annual use of glyphosate in 2025 was noted as 920 000 tons, while about one decade before, in 2014, only 125 000 tons were used.[25] High amounts of this compound are used in agriculture, but also in forestry and urban areas. In general, glyphosate-containing products are applied before traditional agricultural crops are planted or after spreading of genetically modified, glyphosate resistant crops.[17,26–28]

The molecular structure was developed in 1950, but its herbicidal activity was only discovered by John E. Franz in 1970.[26] Four years later, glyphosate was first sold under the trademark name “RoundUp”. The interest in this compound rose drastically and especially with the invention of genetically modified crops (“Round-up ready”).

Glyphosate targets the shikimate pathway, which is required to produce aromatic amino acids along with some secondary metabolites like quinones and folates in plants and many microorganisms.[28,29] In this process, the enzyme 5-enolpyruvylshikimate-3-phosphate synthase (EPSPS) catalyses the synthesis of 5-enolpyruvylshikimate 3-phosphate (**17**, EPSP) by transferring the carboxy-vinyl group from phosphoenolpyruvate (**5**) to the hydroxy group of shikimate 3-phosphate (**15**, S3P) (Scheme 4).[30]

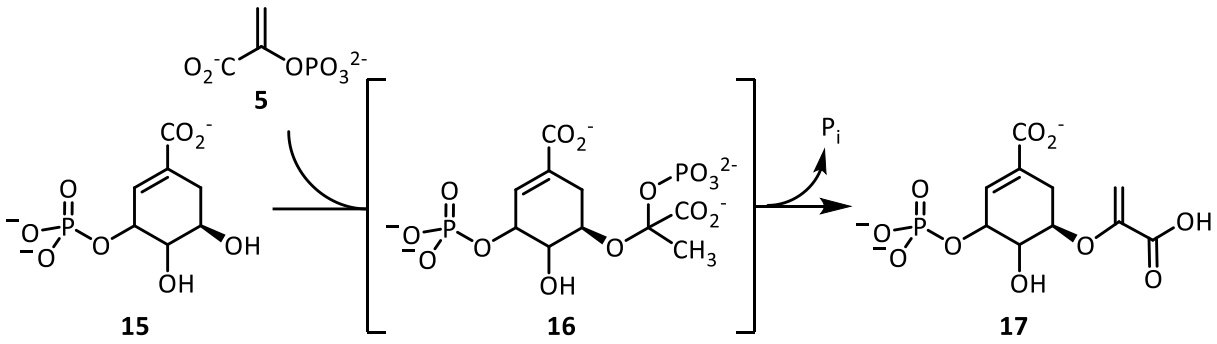

*Scheme 4 – Mechanism of the EPSPS catalysed reaction of S3P (**15**) to EPSP (**17**).*

Glyphosate interacts with EPSPS by mimicking the active oxocarbenium ion intermediate **16**, which is typically formed with PEP by forming a ternary enzyme-glyphosate-S3P complex (**18**, Figure 6).[30,31]

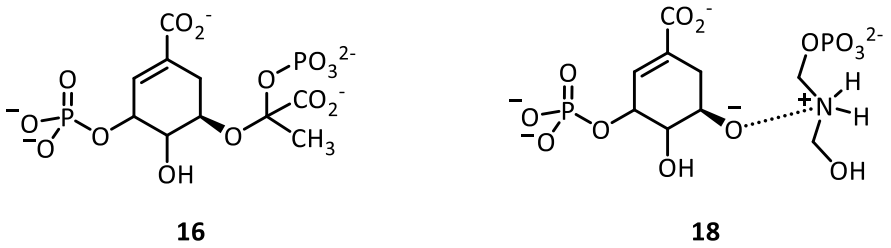

*Figure 6 – Transition state (**16**) of the EPSPS catalysed reaction with S3P and the interaction of glyphosate with S3P (**18**).*

Glyphosate is therefore a reversible, competitive inhibitor for PEP and an uncompetitive inhibitor for S3P.[29] As the extensive use of glyphosate contributed to the accumulation of glyphosate and its metabolites in water and soil throughout the globe, its effects on plants, humans and animals are monitored with concern.[27,32]

Glyphosate gets sold and applied in different compositions, together with various adjuvants. Especially additional surfactants, like polyoxyethylene amine (**19**, POEA), contribute positively to the herbicide uptake and translocation of the active compound into plants. Although glyphosate is quite stable against degradation, it is still metabolised by microorganisms in the soil.[28]

Currently, two biological degradation pathways for glyphosate are known. The first pathway is called AMPA-pathway after its major metabolite aminomethyl phosphonic acid (**20**) and is mediated by a glyphosate oxidoreductase. The flavin-dependent enzyme catalyses the

reaction from glyphosate to **20** and glyoxylate (**21**). AMPA further degrades to methylamine (**22**) and phosphate, a process catalysed by C-P lyase (Scheme 5).[17]

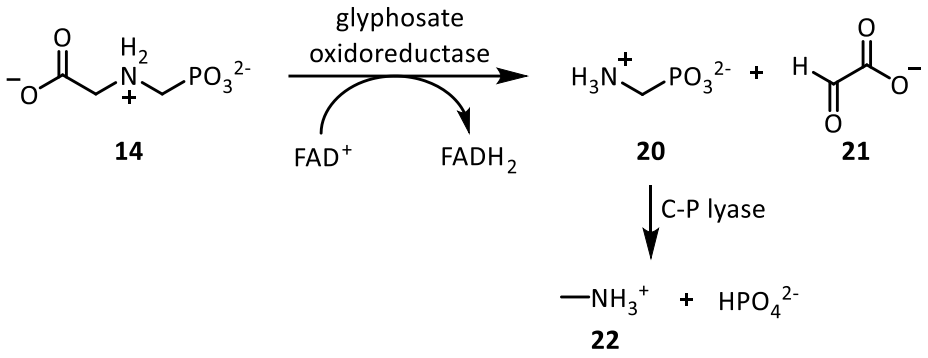

*Scheme 5 – Glyphosate degradation by glyphosate oxidoreductase to AMPA (**20**) and glyoxylate (**21**) and further by C-P lyase to methylamine (**22**) and inorganic phosphate.*

The second pathway is called sarcosine pathway, again like its major intermediate (Scheme 6). In this case, a glyphosate-specific C-P lyase variant cleaves the carbon-phosphorus bond first and produces the intermediates sarcosine (**23**) and phosphate. Sarcosine is further metabolised by sarcosine oxidase under the consumption of water and oxygen to give glycine (**24**) and formaldehyde (**25**). Calculations revealed, that the sarcosine pathway is thermodynamically favoured over the AMPA-pathway, however, microbial cultures tend to degrade *via* the AMPA-pathway.[17,33,34]

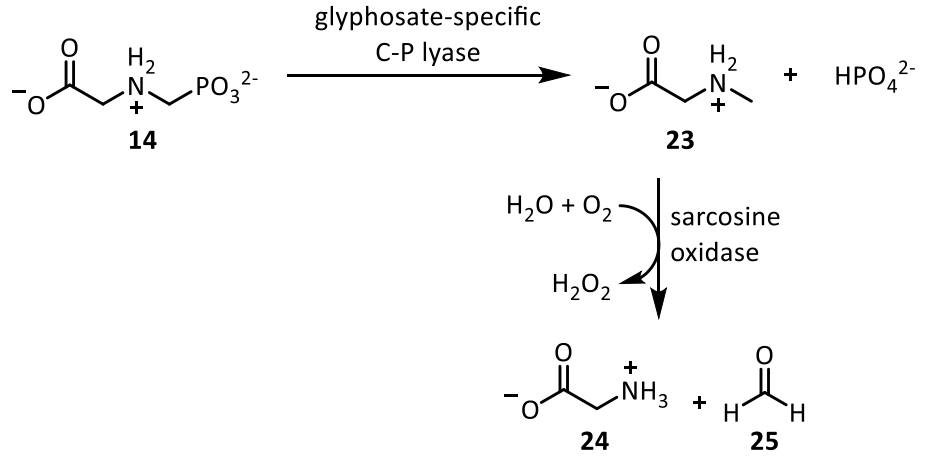

*Scheme 6 – Glyphosate degradation by C-P lyase to give sarcosine (**23**) and inorganic phosphate followed by further degradation to glycine (**24**) and formaldehyde (**25**).*

Both glyphosate and its main degradation product AMPA have severe side effects. While glyphosate induces chlorophyll degradation, AMPA interferes with chlorophyll biosynthesis, resulting in yellowing of the foliage and necrosis of the cells.[28] No further secondary aromatic metabolites like antimicrobial compounds are produced. Thus, glyphosate treated plants often die from infections through commonly present soil pathogens.[28]

The shikimate pathway is not present in humans and animals and therefore glyphosate does not lead to acute toxicity effects in them. However, it can indirectly affect human or animal health. Various correlations between enhanced exposure to glyphosate-containing products and a range of human diseases were found, like links to various forms of cancer[35] and mental conditions such as autism or Alzheimer's disease.[28] Also, miscarriages and dermatological or respiratory illnesses in humans, along with increased infertility or malfunctions in pigs were associated with the increased use of this herbicide.[36,37] Additionally, adjuvants in the herbicidal products can be harmful as well.[28]

The problems arising from glyphosate degradation and accumulation in nature, together with its steadily increasing use, fuel the interest in alternative, new herbicides, with higher specificity and efficiency.

1.5. Pantaphos

A potentially interesting structure in this regard is pantaphos [**26**, 2-(hydroxy[phosphono]methyl)maleate, Figure 7].

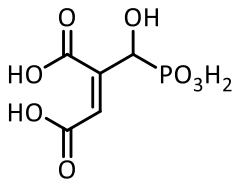

(*Z*)-**26**

Figure 7 – Chemical structure of pantaphos.[38]

Pantaphos (**26**) is a natural product produced by the plant pathogen *Pantoea ananatis.* It is the primary cause of onion center rot, and its biosynthesis is encoded in the *hvr* operon. Moreover, *P. ananatis* also induces various other diseases in crops like rice, corn or wheat.[38,39] Genetically modified *P. ananatis* strains, lacking the ability to produce pantaphos, were studied to proof its role in phytotoxicity. These tests clearly showed that no herbicidal activity is observed using strains that miss the *hvr* operon.

Phytotoxicity assays comparing pantaphos with other P-containing commercially applied herbicides like glyphosate and phosphinothricin revealed a significantly higher potency compared to these.[38,39]

2. Aim of the Thesis

Polidore *et al.* discovered the genes responsible for the introduction of the double bond in pantaphos, which proceeds by a dehydration reaction to give (*Z*)-**26**. However, today no precise information about the absolute configuration of the stereo centre of this compound is available.[38]

Synthetic approaches to access both enantiomers of pantaphos were conducted in the past but until now, only the racemic product could be synthesized. As the stereochemistry is often of high relevance for drug effectiveness, separate studies on the biological effects of the enantiomers of **26**, could provide new insights on its mode of action.[5]

Therefore, this master thesis focused on a stereoselective synthesis of all four potential isomers of the natural product pantaphos [(*S,E*)-**26**, (*S,Z*)-**26**, (*R,E*)-**26**, (*R,Z*)-**26**] as well as the preparation of the saturated analogues (*R*)- and (*S*)-**27** (Figure 8). With those compounds in hands, experiments are planned to determine the three-dimensional structure of the natural product and investigate the structure-activity relationship of these compounds.

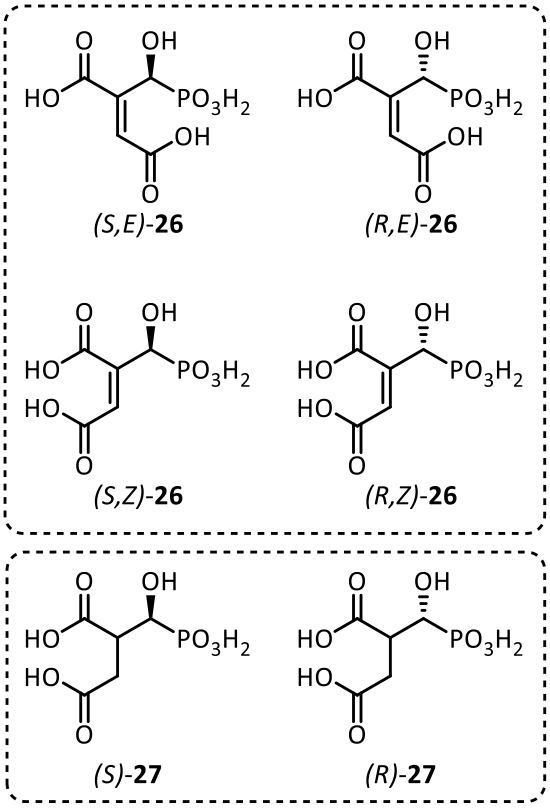

Figure 8 – Target compounds, Upper box: the structures of all possible isomers of pantaphos; Lower box: saturated analogues of pantaphos.

For this purpose, retrosynthetic considerations for the synthesis of the shown pantaphos isomers and their analogues were undertaken. These revealed several possible starting materials leading to the key intermediates **III** and **V** (Scheme 7). The saturated analogues (*R*)- and (*S*)-**27** are envisaged to be obtained similarly, using adapted starting materials.

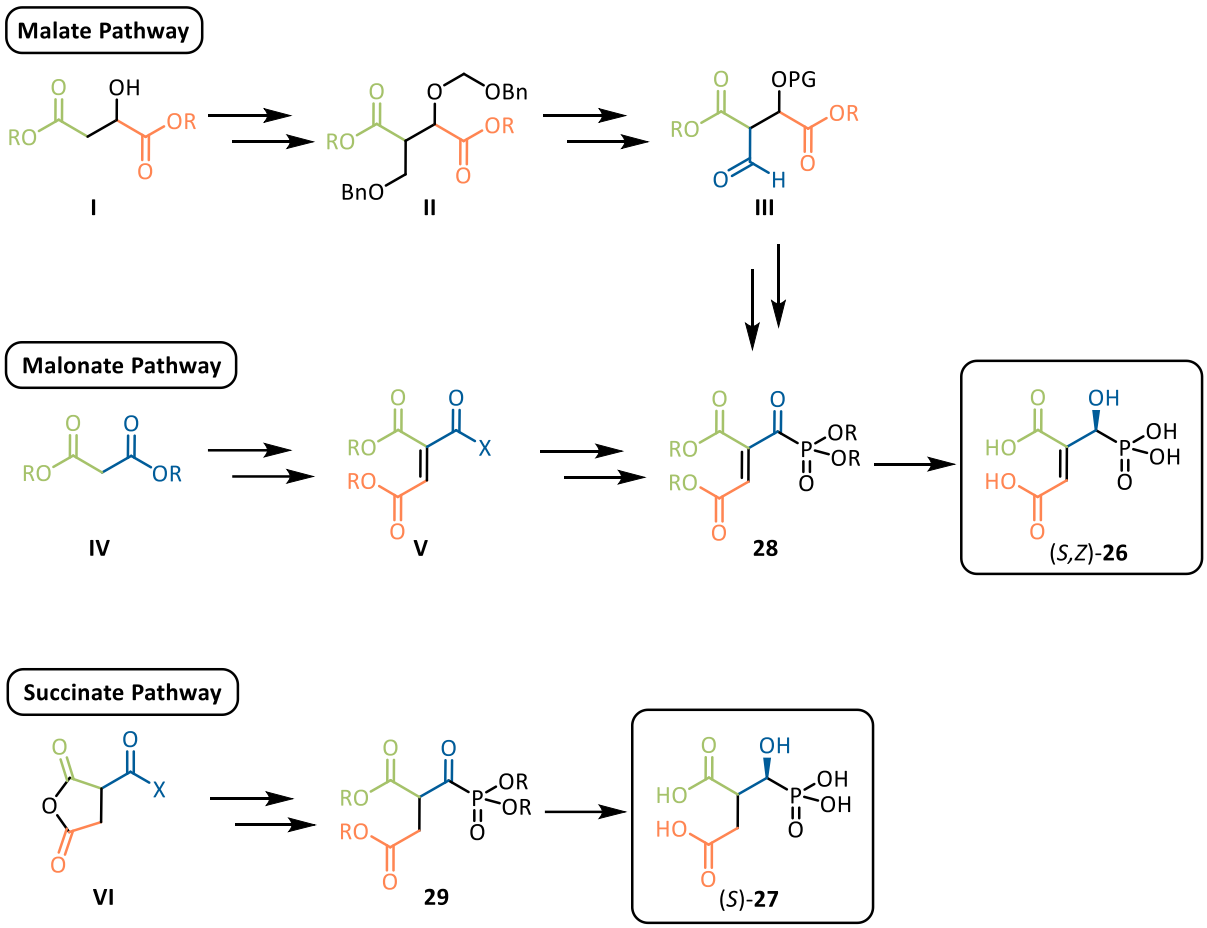

*Scheme 7 – Malate pathway: Synthesis of aldehyde **III** by a Fráter Seebach alkylation with BOMCl starting from dialkyl malate **I** (R = alkyl); Malonate pathway: Synthesis of core structure **V** (X = OR, Cl, H), beginning from dialkyl malonates (**IV**, R = alkyl); Succinate pathway: Synthesis of intermediate **VI** (X = OR, Cl, H) from succinate-based starting materials for the synthesis of (S)-**27**. The respective (R)-enantiomers can be obtained similarly.*

First considerations for the synthesis of **26** from varied malate esters as starting materials were undertaken (Malate pathway, Scheme 7). A Fráter Seebach alkylation of different dialkyl malates (**I**) with benzyl chloro methylether (BOMCl) was envisaged to result in key intermediate **II** which was planned to be converted to the desired intermediate **III** in three steps. The latter was planned to give the protected α-oxophosphonate **28** after the introduction of the phosphonate moiety and elimination of the former malate hydroxy group.

Other ideas included the start from different malonate esters (Malonate pathway, Scheme 7). Various dialkyl malonates (**IV**) can be imagined as adequate starting materials after deprotonation of the active methylene group using bases like *n*-butyl lithium (*n*-BuLi), lithium diisopropylamide (LDA), lithium bis(trimethylsilyl) amide (LHMDS) or different alkoxide. The formed anions were thought to provide core structure **V** by reaction with electrophiles such as ethyl bromoacetate, glyoxylate or allyl halides followed by 2 to 4 manipulation. **V** will finally furnish α-oxophosphonate **28** too.

The third elaborated concept relied on various succinic acid derivatives as starting materials, which were planned to finally yield saturated analogues (*R*)- and (*S*)-**27** (Succinate Pathway, Scheme 7). Here, succinic anhydride or succinate esters were planned to be converted to either an ester, aldehyde or acyl chloride of general structure **VI**, ultimately leading to **29**.

In all three pathways, the C-P bond forming step to give the intermediates **28** and **29** was deemed critical. There is a variety of typical phosphorus-carbon bond forming reactions that can be used to directly generate α-oxo- or α-hydroxy phosphonates.[40,41] The most frequently used α-oxophosphonate forming reaction is certainly the Michaelis-Arbuzov reaction of trialkyl phosphites with acyl halides.[41] As an alternative, the classical Abramov reaction between activated trialkyl phosphites and aldehydes[9], or the Pudovik reaction of dialkyl phosphites in combination with a base and an aldehyde can be generally used for the formation of racemic α-hydroxy phosphonates.[43]

All three reactions could be used to build up the desired C-P bond and can thus (in two cases after oxidation) result in an α-oxo-phosphonate like **28**. The latter was subsequently planned to be stereoselectively reduced *via* asymmetric transfer hydrogenation (ATH). During the course of this thesis, classical Noyori-type catalysts were planned to be used here for the formation of the desired stereo centre. Depending on the used catalyst-configuration, either *(R,R)*- or *(S,S)*-RuCl[(*p*-cymene Ts-DPEN] [(*R,R*)-or (*S,S*)-**30**, Figure 9], the reduction was planned to give (*S*)- or (*R*)-configured, protected pantaphos, respectively.[44]

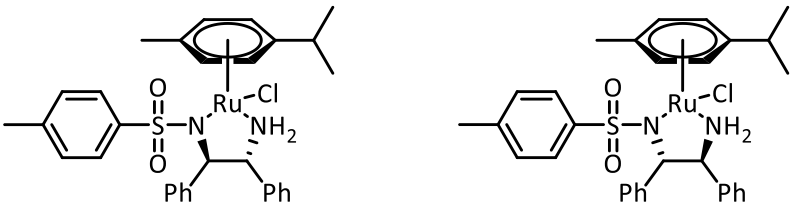

(R,R)-**30** *(S,S)*-**30**

Figure 9 – Structure of the used Noyori-type catalysts for the planned ATH.

3. Results and Discussion

Pantaphos has been successfully isolated from the plant bacterium *Pantoea ananantis* by Polidore *et al.* and was chemically synthesized in the past, albeit only as a racemic mixture of both possible geometric isomers.[5,45] Because of the future potential applications of pantaphos and the gaps in knowledge about its biosynthesis, different approaches for the stereoselective synthesis of all possible isomers of **26** and of both enantiomers of **27** were tested.

3.1. Synthesis Route 1

The first tested route to access (*R*)- and (*S*)-**26** started with commercially available malic acid (**31**), which was esterified under acidic conditions (Scheme 8).

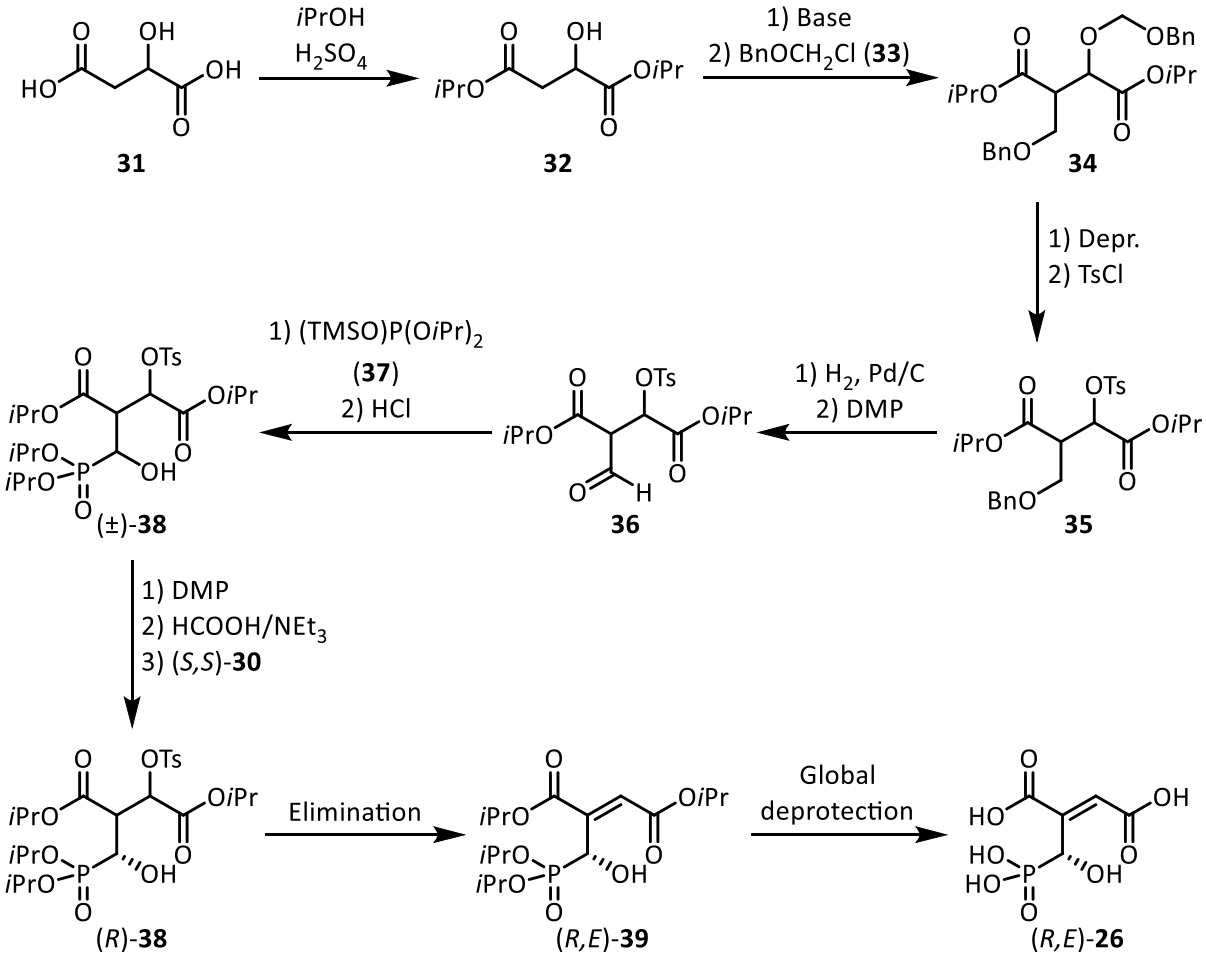

*Scheme 8 – Synthesis route 1 towards (R)-**26**, exemplified for diisopropyl malate as starting material. The (S)-enantiomer can be obtained similarly. ATH = asymmetric transfer hydrogenation, DMP = Dess-Martin periodinane.*

The obtained diisopropyl malate (**32**) was then planned to be subjected to a Frater-Seebach-type alkylation with BOMCl (**33**). Next, a removal of the methoxybenzyl-group, followed by tosylation of the formed intermediate was planned to give **35**. Subsequently, hydrogenation in the presence of palladium on carbon was envisaged, followed by oxidation of the resulting primary alcohol using Dess-Martin periodinane. The resulting aldehyde **36** was planned as starting material for an Abramov-type reaction with the activated trialkyl phosphite **37** which would result in the formation of the racemic α-hydroxy phosphonate (±)-**38**. The latter needs to be oxidized for a subsequent asymmetric transfer hydrogenation in the presence of a Noyori-type catalyst. Depending on the used catalyst configuration, either the (*R*)- or (*S*)-enantiomer of **38** will be formed. Elimination of the tosyl-protected hydroxy group and final global deprotection under acidic conditions was planned to form the desired double bond and finally yield **26**.

While both diethyl- and diisopropyl malate (**32**) were easily accessible in 95 % and quantitative yield, respectively, the subsequent steps did not proceed with the same efficiency. The described Fráter Seebach alkylation suffered from low overall yields regardless of parameters such as temperature, reaction time, solvent or varied additives. However, using **32** as substrate gave better results (37 % yield) compared to diethyl malate. Hence, diisopropyl malate (**32**) was used for the optimization of all subsequent steps, as it is also literature known to be more stable under the needed reaction conditions.[46]

Frater Seebach alkylations are commonly performed using the highly toxic additive HMPA (hexamethyl phosphoric triamide) for stabilization of the formed primary carbocations.[47] In order to avoid its use, different polar aprotic additives were tested as shown in Table 1.

*Table 1 – Tested additives for the Fráter Seebach alkylation of **33** with BOMCl. r.t. = room temperature, n.d. = not detected.*

Entry	Additive	Conditions	Isolated yield of 34
1	ACN	−50 °C, 5h	37 %
2	ACN	−50 °C, 4 h → r.t. 16 h	25 %
3	DMF	−50 °C, 2 h → r.t. 14 h	24 %
4	THF	−50 °C, 2 h → r.t. 14 h	13 %
5	DMPU	−50 °C, 4 h → r.t. 17 h	n.d.

1 mL of additive was used per mmol educt before the addition of BOMCl. Despite the known ability of DMPU to replace HMPU as an additive in Fráter Seebach alkylations, no product formation was observed in this case (entry 5). Additionally, DMF (entry 3) and THF (entry 4) were tested as polar aprotic additives. In both cases the functionalized diisopropyl malate **34** was obtained, but with low yields of 24 % and 13 % yield, respectively.

The best results were observed in the presence of acetonitrile (entry 1). Comparing different reaction temperatures and times revealed that shorter reaction times and lower temperatures (compare entry 1 and 2) are beneficial. After 5 hours at −50 °C, a yield of 37 % could be isolated. This hints at a low stability of **34** under highly basic conditions at elevated temperatures.

The yield of the conducted Fráter-Seebach alkylation could be dramatically increased by fine tuning of the reaction conditions and structural changes in the starting material (replacing ethyl by isopropyl residues), but all attempts consistently yielded **40** as major byproduct, along with unreacted BOMCl (Figure 10).

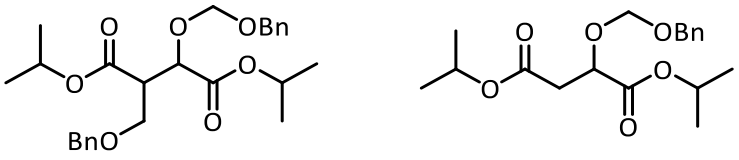

34 **40**

*Figure 10 – Products of the conducted Fráter Seebach alkylations; desired product **34**, major byproduct **40**.*

Tests to replace *n*-BuLi by LDA as a base for the attempted *C*-alkylation of **32** were conducted at −50°C and using ACN as additive. Unfortunately, this led to elimination of the hydroxy group.

Despite the low overall yields, having **34** in hands, several attempts for the needed *O*-deprotection were executed (Table 2).

*Table 2 – Tested conditions for the deprotection of the BOM ether of **34**.*

Entry	Reagent	Solvent	Conditions	Isolated yield
1	$BF_3 \times OEt_2$	ACN	0 °C → r.t., 24 h	17 %
2	DOWEX H^+	MeOH	65 °C, 3 days	n.d.
3	aq. HCl	1,4-Dioxane	60 °C, 60 h	13 %
4	aq. HCl	THF	r.t., 60 h	14 %
5	HCl in Dioxane	1,4-Dioxane	r.t., 16 h, then 6 days reflux	11 %
6	TMSCl	MeOH	r.t., 22 h, then 26 h at 40°C	16 %

First attempts with hydrochloric acid and methanol were conducted as described by Ueki *et al*.[48] This procedure worked once with a yield of 17 %, but lacked reproducibility as the following four attempts did not yield any product at all. Other approaches with boron trifluoride, hydrochloric acid in either 1,4-dioxane or THF, as well as trimethylsilyl chloride (TMSCl) in methanol yielded the desired deprotected product, although in low yields between 11 % and 17 %. Attempts with DOWEX® 50W (H^+-form) in methanol as H^+ source failed completely.

Due to the consistently low yields in all but the first step of this synthetic route, other strategies were tested.

Due to difficulties in the selective deprotection of the BOM ether, attempts to use *O*-protected substrates for the intended Fráter-Seebach-like alkylation were investigated too. Both mesylated- and tosylated malates **41** and **43** were successfully synthesized for this purpose in 29 % and 40 %, respectively (Scheme 9).[49] Tosylation using *para*-toluene sulfonyl chloride (*p*-TsCl) was tested in pyridine at 0°C, but only led to re-isolation of the starting material.[50] Similar results were observed with sodium hydroxide in a mixture of THF and water.[51] The products could finally be successfully synthesized using toluene as solvent and tetramethyl ethylene

diamine (TMEDA) as base at 0°C.[49] Unfortunately, the *C*-alkylation of the methylene group in **41** and **43** could not be achieved under typical conditions for Fráter Seebach alkylation using BOMCl as electrophile.

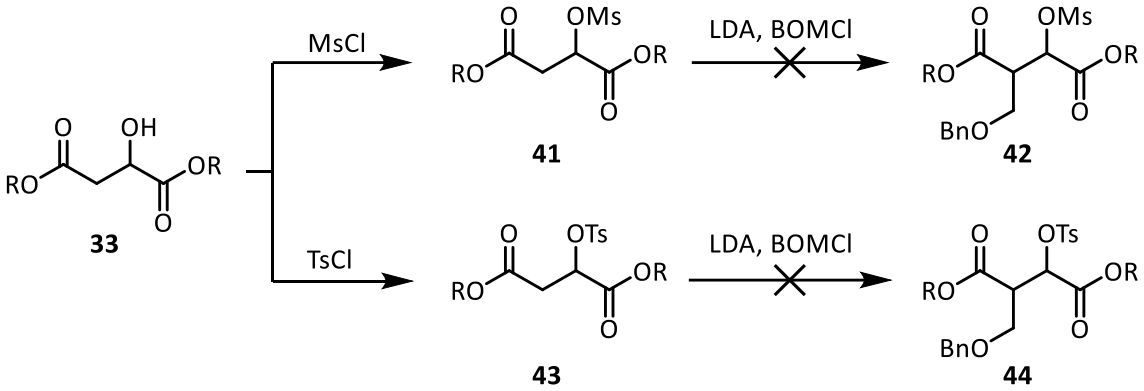

Scheme 9 – Synthesis of mesylated and tosylated starting materials for the attempted C-alkylation.

3.2. Synthesis Route 2

As neither of the attempted Fráter Seebach alkylations delivered the desired product in satisfying yields, another strategy was developed, starting from ethyl malonyl chloride [(**45**), Scheme 10].

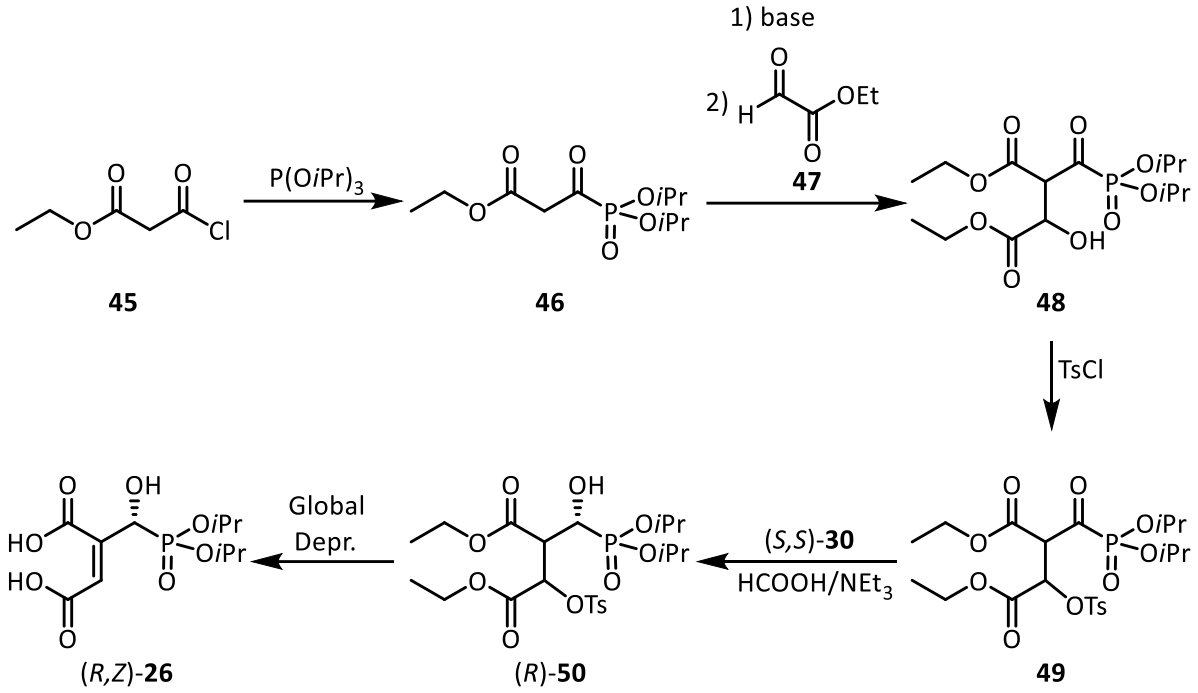

*Scheme 10 – Planned synthesis route 2, exemplified for the synthesis of (R,Z)-**26**; the respective (S)-enantiomer can be obtained similarly.*

An Arbusov reaction starting from ethyl malonyl chloride (**45**), followed by deprotonation and addition of ethyl glyoxylate to the resulting carbanion was attempted to give **48**.

For this purpose, ethyl glyoxylate (**47**) first had to be synthesized through ozonolysis of diethyl fumarate (**51**). This proceeded in 68 % yield (Scheme 11).

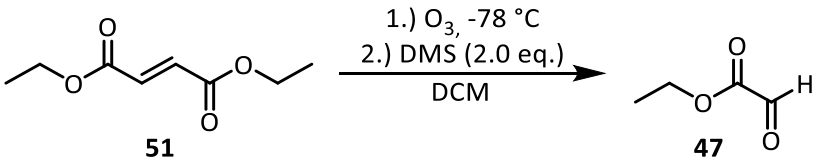

Scheme 11 – Ozonolysis of diethyl fumarate to yield ethyl glyoxylate.

Although **47** was distilled (25 mmHg, 48 °C) to remove the side product (DMSO) and its partially formed polymer, traces of both were still present in the final product. It is noteworthy

to mention that storage at lower temperatures significantly slows down the polymerization process. Therefore, storage of **47** is only possible for a few days at −20°C.

The subsequent protection of the formed hydroxy group in **48** was planned prior to the stereoselective reduction of the carbonyl group next to the phosphorus atom. An ATH was again envisaged for stereoinduction, followed by elimination and global deprotection under acidic conditions to obtain the final product **26**.

According to literature, α-oxo-phosphonate **46** was formed in an Arbusov reaction.[52] The reaction was shown to be finished within one hour by ^{31}P NMR. Removal of volatile byproducts (diisopropyl phosphite) and remaining starting material (triisopropyl phosphite) from the reaction mixture worked best at 50 °C and 0.5 mbar for approximately one hour. No purification was necessary at this stage and the product was obtained in quantitative yield.[52]

Then, deprotonation of the active methylene compound was accomplished with sodium hydride (NaH) and ethyl glyoxylate was added at 0 °C to the reaction mixture. Unfortunately, proton NMR revealed complete loss of the isopropyl-protecting groups under the chosen conditions.

Hence, the planned ATH was tested first with **46** to obtain the according hydroxy phosphonate (*S*)-**52** (Scheme 12).

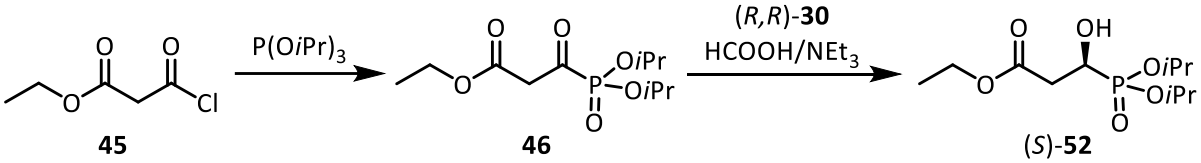

*Scheme 12 – Synthesis of (S)-**52**; the (R)-enantiomer can be obtained similarly by using (S,S)-**30**.*

The latter was planned to be subjected to a Fráter-Seebach alkylation. Both, (*S*)- and (*R*)-**52** were accessible by the ATH of **46** in the presence of either (*R,R*)-**30** and (*S,S*)-**30**, respectively. The reaction could be monitored by NMR [δ_P(**46**) −3.5 ppm; δ_P(**52**) 20 ppm]. Determination of the enantiomeric excess (ee) of the product and an estimation of the obtained configuration could be accomplished by the use of a chiral solvating agent (**53**, Figure 11).

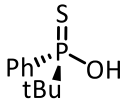

53

*Figure 11 – Chemical structure of (S)-(-)-tert-butylphenylphosphinothioic acid [(S)-**53**].*

As described by Drescher *et al.*, the signals of the formed complexes of (*S*)-(-)-*tert*-butylphenylphosphinothioic acid with (*R*)-hydroxyphosphonates tend to shift to lower field in ^{31}P NMR spectra while the respective signal of the α-proton next to the phosphorus is shifted to higher field in proton NMR spectra.[53] (*S*)-Enantiomers tend to behave conversely, resulting in a high field signal-shift in ^{31}P NMR and a low field signal-shift for the signal of the α-proton in presence of this particular chiral solvating agent (Figure 12 and Figure 13).

Using this method showed both compounds to be enantiopure (ee ≥ 99%) and their absolute configuration to be presumably in line with the presented hypothesis of (*S,S*)-**30** giving (*R*)-hydroxy-phosphonates and *vice versa*.

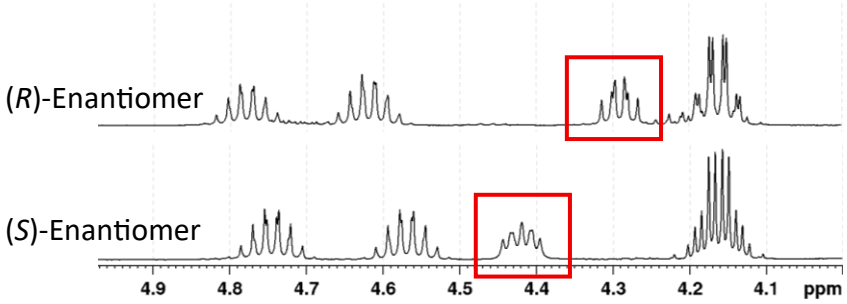

*Figure 12 – Comparison of proton NMR spectra of (R)-**52** (top) and (S)-**52** (bottom) in the presence of chiral solvating agent (S)-(-)-tert-butylphenylphosphinothioic acid [(S)-**53**].*

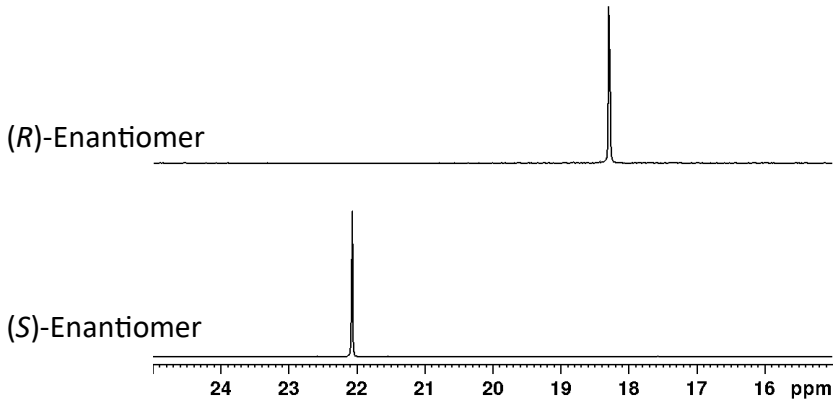

*Figure 13 – ^{31}P NMR spectra of (R)-**52** (top) and (S)-**52** (bottom), each in presence of chiral solvating agent (S)-(-)-tert-butylphenylphosphinothioic acid [(S)-**53**].*

With the obtained hydroxyphosphonate **52** in hands, the addition of ethyl glyoxylate was tested again, as previously described starting from oxo-phosphonate **46**. Deprotonation of **52** with LDA at −50 °C, followed by addition of ethyl glyoxylate did not lead to the desired product.

Thus, varied other electrophiles and different bases were tested both starting from oxo-phosphonate **46** and hydroxy phosphonate **52** (Scheme 13 and Table 3).

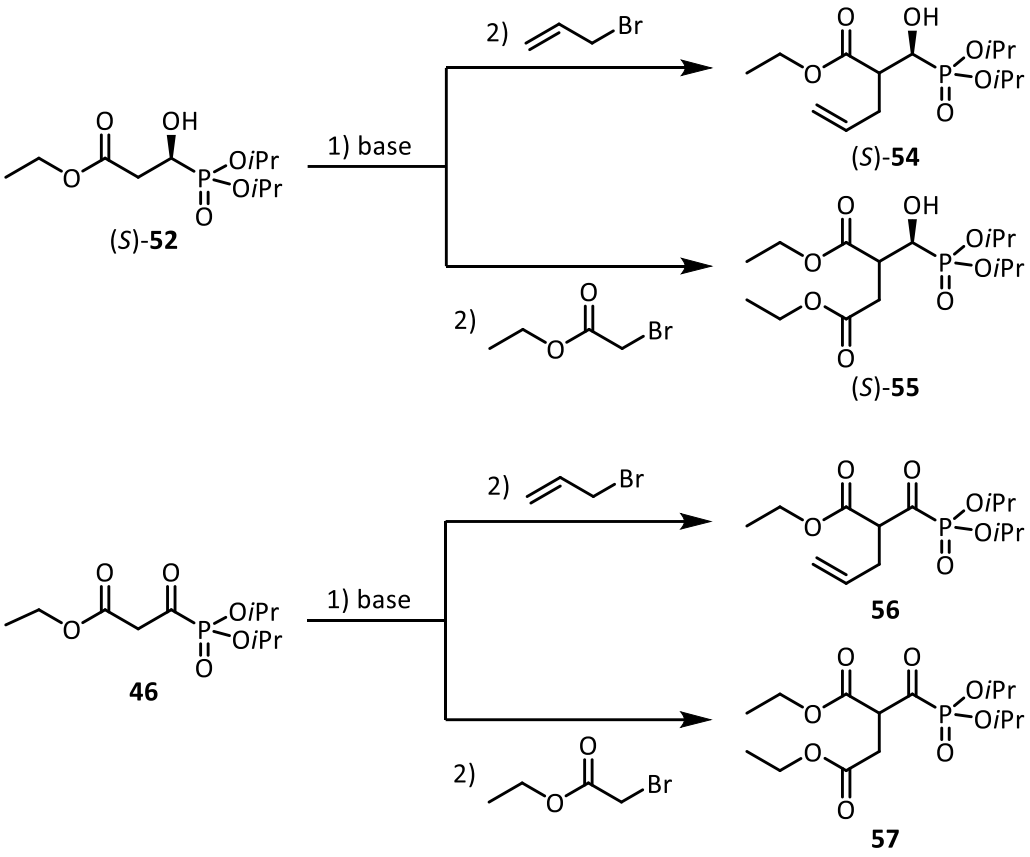

*Scheme 13 – Tested alkylations to obtain key intermediates **54-57**.*

*Table 3 – Bases and electrophiles tested for the synthesis of **54**-**57**. decomp = decomposition. s.m. = starting material.*

Entry	Starting material	Base	Electrophile	Temp /°C	Isolated
1	**46**	NaH	allyl bromide	−50	decomp.
2	**46**		ethyl bromoacetate	−50	
3	**46**	NaOEt	allyl bromide	0	decomp.
4	**46**		ethyl bromoacetate	0	
5	**46**	NaOEt	allyl bromide	−50	s.m.
6	**46**		ethyl bromoacetate	−50	6 % of **58** or **59**
7	**52**	LHMDS	allyl bromide	−50	s.m.
8	**52**		ethyl bromoacetate	−50	3 % of **55**
9	**52**	*n*-BuLi	allyl bromide	−50	s.m.
10	**52**		ethyl bromoacetate	−50	4 % of **55**
11	**52**	*n*-BuLi	CH_3I	−40	s.m.

Bases like sodium hydride (NaH) (entry 1 and 2) and sodium ethoxide (NaOEt) (entry 3-6) were tested for deprotonation of compound **46**, while LHMDS (entry 7 and 8) and *n*-BuLi (entry 9, 10 and 11) were tested in combination with **52**. Deprotonation oxo-phosphonate **46** worked best with NaOEt at low temperatures (−50 °C) (entry 5 and 6), as judged by proton NMR. NaH led to decompositions at the tested temperature (0 °C). Deprotonation of compound **52** worked both using LHMDS and *n*-BuLi, but again, low temperatures (below −40 °C) were necessary to guarantee the stability of the intermediate anion.

After deprotonation, varied electrophiles were added. Attempts with allyl bromide as electrophile did not show product formation. Using ethyl bromoacetate as electrophile led to addition in three cases (entry 6, 8 and 10), albeit product purification proved difficult in all of them. Purification of the reaction mixture of entry 6 proved to be intricate in typical mobile phase mixtures, thus it was performed in a mixture of toluene and acetone. The isolated compound lacked one ethyl group and was only formed in 6 % yield, (Figure 14).

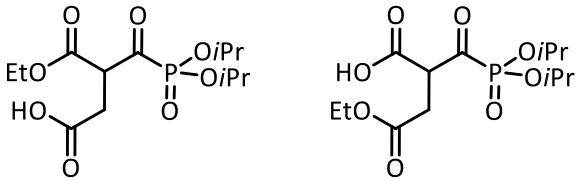

58 **59**

*Figure 14 – Possible product structures isolated from the reaction of **52** with ethyl bromoacetate.*

LHMDS (entry 8) yielded 3 % of **55** after one hour at −78 °C, compared to 4 % with a molar purity of 51 % (judged by NMR) when using *n*-BuLi at −50 °C (entry 10). In both cases, reaction work-up was conducted similarly (an acidic quench and an aqueous work up followed by column chromatography). Subsequently, additional column chromatographic purification attempts were performed. First, a mixture of *n*-heptane and ethyl acetate (detailed information available in experimental part) was tested, followed by a mixture of CH_2Cl_2 and acetone (6:1). Unfortunately, compound purity declined after each purification attempt as judged by proton NMR, which hinted at compound degradation. This is assumed to be related to the use of slightly acidic silica gel as stationary phase. Thus, the chosen acidic work-up might also have caused significant product degradation. Future purification attempts will focus on the optimization of the quenching conditions, and the use of slightly basic solvents or alternative stationary phases for purification to solve this problem.

In order to prove the principal feasibility of the approach, the generated anion was reacted with methyl iodide as electrophile, due to its known ability to easily undergo Fráter Seebach type alkylations, albeit without success (Table 3, entry 11 and Scheme 14).

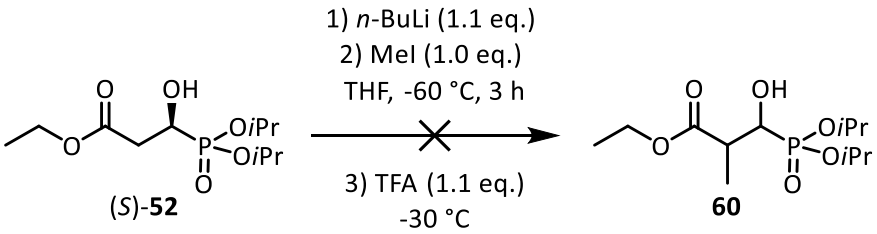

*Scheme 14 – Reaction of compound **52** with nBuLi and MeI.*

Because of time constraints, the conclusions from these experiments could not be used for further synthesis optimization. Future attempts for the synthesis of **26** will focus on these and explore the Fráter Seebach alkylation of **52** with BOMCl, e.g.

3.3. Synthesis Route 3

A third synthesis route (Scheme 15) was designed starting from diethyl malonate (Malonate pathway in Scheme 7).

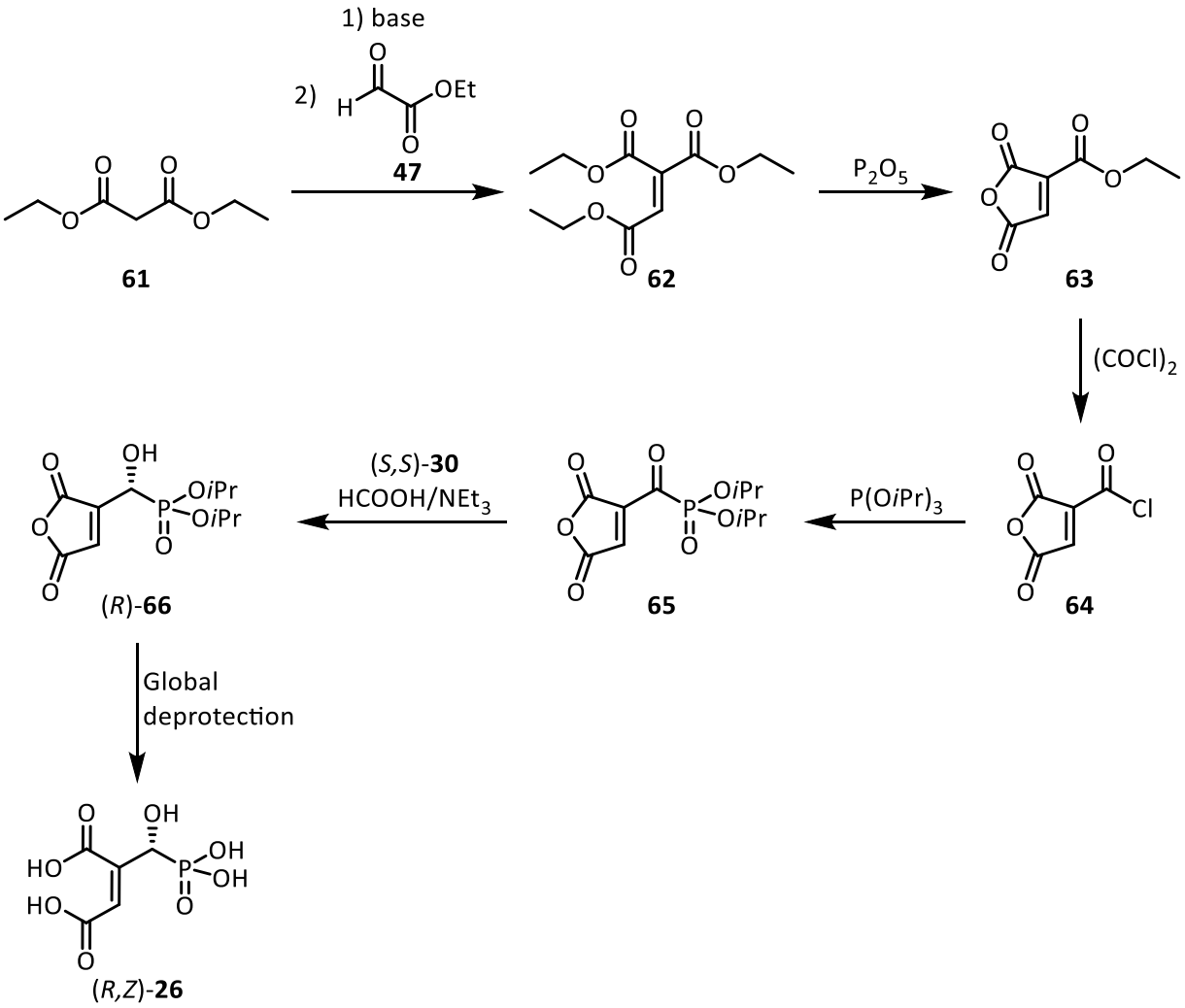

*Scheme 15 – Planned synthesis route 3 to obtain **26**, exemplified for the (R)-enantiomer.*

The latter was planned to give triester **62** in a Knoevenagel-type condensation, followed by a ring closure with phosphorus pentoxide. **63** was then further planned to be converted to acyl chloride **64** which could be subjected to an Arbusov reaction with trialkyl phosphite. Then, an ATH was planned to furnish (*R*)- or (*S*)-**66**. Global deprotection under acidic conditions was planned to complete the synthesis route and yield the desired product in (*R*,*Z*)- or (*S*,Z)-configuration.

Triethyl ethene tricarboxylate (**62**) was successfully obtained in 38 % yield by a literature known procedure.[54] The planned ring closure with phosphorus pentoxide (P_2O_5) was attempted at 160 °C for 5 hours, but no product formation was detected after aqueous work up. This was assumed to be due to the tendency of maleic anhydride to hydrolyse in presence of water.[55] Thus, another cyclisation approach was tested using trifluoroacetic acid (TFA) in order to avoid a subsequent need for an aqueous workup.[56] The reaction was monitored for three days but no product formation was observed.

3.4. Synthesis Route 4

As the attempted ring closure to yield **63** proved challenging, an approach directly starting from commercially available, succinic anhydride (**67**) was tested.

In a first attempt, diethyl formyl phosphonate (**68**) was planned to react with succinic anhydride after deprotonation with LDA at −78°C (Scheme 16).

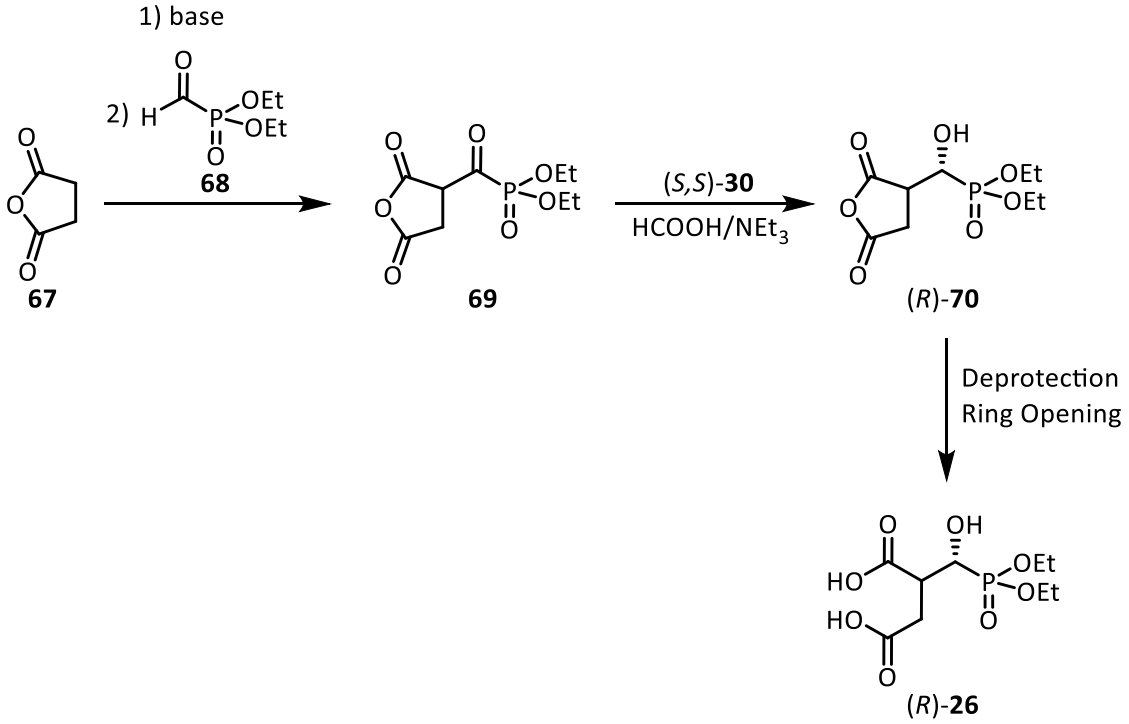

*Scheme 16 – Planned synthesis route 4 to obtain the product (R)-**26**, the (S)-enantiomer can be obtained similarly.*

68 was synthesized by ozonolysis of diethyl vinyl phosphonate (**71**), with a purity of 39 mol% only and was directly used for the next step without further purification or solvent removal.

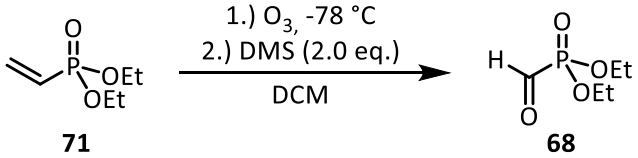

*Scheme 17 – Ozonolysis of **71** to give **68**.*

68 was added to succinic anhydride after deprotonation at −78 °C in the presence of LDA. Unfortunately, only degradation was observed. As formyl phosphonates are known to be

highly unstable at room temperature, its stability and the low purity might have caused the failure to synthesize **69**.[57]

Next, the addition of diethyl formyl phosphonate to maleic anhydride was tested. Maleic anhydride easily undergoes Diels-Alder-reactions, Friedel-Crafts acylations or esterifications, to name but a few.[58] This reaction was attempted at −78 °C. As no reaction was observed at this temperature (judged by NMR), the temperature was gradually raised to −20 °C and then to 0°C with no effect. In the future, higher temperatures and alternative procedures for the addition will be tested.

4. Experimental Part

4.1. General Experimental Part

The used chemicals were obtained from abcr chemicals, Acros, BLDpharm, Euroisotop, Fluka, Merck, Sigma-Aldrich, Thermo Fisher Scientific and Tokyo Chemical Industry (TCI).

Thin layer chromatography (TLC) was performed with Merck silica gel 60 F_{254} glass plates (0.25 mm thick coating). Visualization of product spots was conducted using UV light (254 nm) and/or the stains described below:

- Vanillin stain: 15 g vanillin in 250 mL ethanol and 2.5 mL H_2SO_4 (conc.)
- Cerium ammonium molybdate (CAM)-stain: 46 g $(NH_4)_6Mo_7O_{24}$ × 4 H_2O and 2 g $Ce(SO_4)_2$ × 4 H_2O in 1 L 10 % H_2SO_4
- $KMnO_4$ stain: 9 g $KMnO_4$ in 900 mL H_2O and 15 mL 5 % aq. NaOH

Chromatographic purifications were performed on a fully automated Biotage Isolera Prime™ flash purification system. The separation cartridges were either pre-packed Biotage® Sfär Duo separation cartridges with 5 to 350 g silica or self-filled Sfär-Duo cartridges with Macherey-Nagel silica gel 60 (230-400 mesh).

NMR-spectra were recorded using the following Bruker devices:

- BioSpin AV III HD 700 (^{1}H: 700.40 MHz, ^{13}C: 176.12 MHz)
- AV III 600 (^{1}H: 600.25 MHz, ^{13}C: 150.93 MHz, ^{31}P: 242.99 MHz)
- AV NEO 400 (^{1}H: 400.27 MHz, ^{13}C: 100.65 MHz, ^{31}P: 162.03 MHz)
- AV NEO NanoBay 400 (^{1}H: 400.13 MHz, ^{13}C: 100.61 MHz, ^{31}P: 161.98 MHz)

Compound purities are given in mol% and are estimated based on ^{1}H or ^{31}P spectra. If not further specified, compound purity was estimated as >99 mol%.

The recorded spectra were referenced as listed in Table 4.

Table 4 – Solvent (residual) peaks used as references for the recorded NMR spectra.

Nucleus	Solvent	Referenced to (residual)	Shift/ppm
^{1}H	$CDCl_3$	$C\mathbf{H}Cl_3$	7.26
	D_2O	**H**OD	4.79
^{13}C	$CDCl_3$	$\mathbf{C}DCl_3$	77.16
^{31}P	External H_3PO_4	$H_3\mathbf{P}O_4$	0.00

Mass spectra were recorded using electrospray ionization (ESI) either on a Thermo Scientific Ultimate 3000 RSLCnano system with capillary flow or a Thermo Scientific Ultimate 3000 HPLC system coupled with a Bruker maXis ultra-high-resolution time-of-flight (UHR-TOF) detector.

4.2. General Procedures

4.2.1. General Procedure A: Preparation of lithium diisopropyl amide

n-Butyl lithium (2.5 M in *n*-hexanes, 1.0 eq.) is added to a cooled solution of diisopropyl amine (1.2 eq.) in dry THF (5 mL/mmol) at −78 °C under argon. The resulting mixture is stirred for 30 minutes at the same temperature.

4.2.2. General Procedure B: Activation of (*R,R*)- or (*S,S*)-**30**

An aqueous solution of potassium hydroxide (0.2 M, 1.0 eq.) is added to a stirred solution of (*R,R*)- or (*S,S*)-RuCl[(*p*-cymene) Ts-DPEN] [(*R,R*)- or (*S,S*)-**30**, 0.02 mmol, 12.4 mg] in CH_2Cl_2 (1 mL / 100 mg). The biphasic mixture is stirred vigorously for 2-3 minutes, during which the colour changes from orange to purple. The phases are separated, the organic phase is washed twice with water and dried over CaH_2. After gas evolution ceases, the catalyst solution is filtrated through a cotton plug. The activated catalyst solution can be either used directly or stored under argon at −20°C for approximately 7 days.

4.2.3. General Procedure C: Asymmetric Transfer Hydrogenation

Formic acid (4.4 eq.) is added dropwise to triethylamine (2.6 eq.) at 0 °C under argon and the resulting mixture is stirred for five minutes. The respective carbonyl compound (1.0 mmol, 1.0 eq.) is meanwhile dissolved in CH_2Cl_2 (2 mL / mmol) under argon. The mixture of formic acid and triethylamine is added slowly to the latter, followed by a solution of the activated catalyst (*R,R*)- or (*S,S*)-**30** (0.01 – 0.05 eq. as specified) in dry CH_2Cl_2 (1 mL /100 mg, final concentration of 0.16 M) is added. The solution is heated to 35 °C and stirred for the indicated time. The solvent is evaporated *in vacuo,* and the residue purified as described for each compound.

4.3. Syntheses

4.3.1. Synthesis of (±)-diethyl malate (**72**)

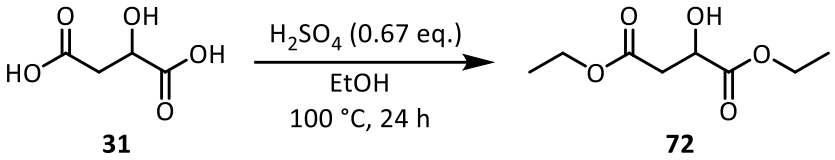

Malic acid (**31**, 12.47 g, 93.0 mmol, 1.0 eq.) and concentrated sulfuric acid (3.5 mL, 63.0 mmol, 0.67 eq.) were dissolved in 200 mL ethanol. After refluxing for 24 hours the mixture was allowed to reach room temperature and was concentrated *in vacuo*. CH_2Cl_2 (150 mL) was added, and the organic phase was washed with a saturated aq. $NaHCO_3$ solution until neutral. The organic phase was dried over $MgSO_4$, and the solvent was removed under reduced pressure. Product **72** was obtained as a slightly yellowish oil (16.8 g, 88.2 mmol, 95 % yield).

$\mathbf{R_f}$ (*n*-heptane:EtOAc = 3:2) = 0.3 ($KMnO_4$)

^{1}H NMR (400.27 MHz, $CDCl_3$, [41Sep1725/240]): δ_H: 4.48 (dd, J_{AX} = 4.5 Hz, J_{BX} = 6.0 Hz, 1H, CH), 4.27 (dq, J_{HH} = 2.4 Hz, J_{HH} = 7.2 Hz, 2H, C**H**$_2$-CH_3), 4.17 (q, J_{HH} = 7.2 Hz, 2H, C**H**$_2$-CH_3), 3.32 (broad s, 1H, OH), 2.82 (ABX-system, A part: dd, J_{AB} = 16.4 Hz, J_{AX} = 4.5 Hz, B part: dd, J_{AB} = 16.4 Hz, J_{BX} = 6.0 Hz, 2H, CH_2), 1.30 (t, J_{HH} = 7.2 Hz, 3H, -CH_2-C**H**$_3$), 1.27 (t, J_{HH} = 7.2 Hz, 3H, -CH_2-C**H**$_3$) ppm.

4.3.2. Synthesis of (±)-diisopropyl malate (**32**)

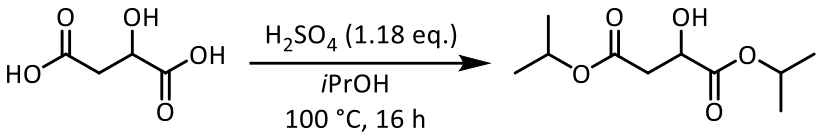

31 **32**

Malic acid (**31**, 14.0 g, 110.0 mmol, 1.0 eq.) and concentrated sulfuric acid (7.22 mL, 130.0 mmol, 1.18 eq.) were dissolved in isopropanol (11.5 mL) and refluxed for 16 hours at 100 °C. The solvent was evaporated *in vacuo,* the residual liquid was taken up in CH_2Cl_2 and washed with a sat. aq. $NaHCO_3$ solution until neutral. The organic phase was dried over $MgSO_4$ and the solvent was removed under reduced pressure to obtain **32** as a colorless oil (3.95 g, 90 % yield).

R_f (*n*-heptane:EtOAc = 3:2) = 0.5 (CAM)

^{1}H NMR (400.27 MHz, $CDCl_3$, [42Sep2225/110]): δ_H: 5.3 (s, impurity: CH_2Cl_2, ∫0.12), 5.12 (sept, J_{HH} = 6.3 Hz, 1H, CH *i*Pr), 5.04 (sept, J_{HH} = 6.3 Hz, 1H, CH *i*Pr), 4.42 (ddd, J_{AX} = 4.7 Hz, J_{BX} = 5.7 Hz, $J_{X,OH}$ = 5.5 Hz, 1H, CH), 3.20 (d, $J_{X,OH}$ = 5.5 Hz, 1H, OH), 2.77 (ABX, A part: dd, J_{AB} = 16.3 Hz, J_{AX} = 4.7 Hz, B part: dd, J_{AB} = 16.3 Hz, J_{BX} = 5.7 Hz, 2H, CH_2), 1.28 (d, J_{HH} = 6.3 Hz, 3H, 1 × *i*Pr), 1.58 (s, impurity: H_2O, ∫0.18), 1.27 (d, J_{HH} = 6.3 Hz, 3H, 1 × *i*Pr), 1.24 (d, J_{HH} = 6.3 Hz, 6H, 2 × *i*Pr) ppm.

4.3.3. Synthesis of diisopropyl 2-(benzyloxy)-3-((benzyloxy)methoxy)succinate (**34**)

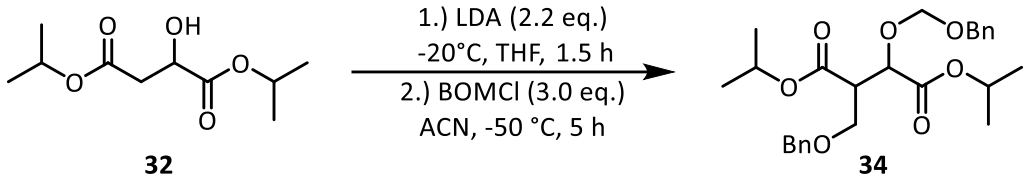

32 **34**

Diisopropyl malate (**32**, 0.44 g, 2.0 mmol, 1.0 eq.) dissolved in dry THF (2 mL) was added to a solution of LDA (prepared by general procedure **A**, 4.4 mmol, 2.2 eq.) in THF at −20 °C and the resulting mixture was stirred for 1.5 hours. Then, the solution was cooled to −50°C and benzyl chloromethyl ether (**33**, 1.39 mL, 90%, 6.0 mmol, 3.0 eq.) dissolved in dry acetonitrile (4 mL) was added over a period of 20 minutes. After 5 hours at this temperature, a solution of glacial acetic acid and diethyl ether (4:5, 9 mL) was added. The reaction mixture was then poured into water and extracted thrice with diethyl ether. The combined organic phases were dried ($MgSO_4$), concentrated and the residue purified by column chromatography (100 g silica, gradient of EtOAc in *n*-heptane: 1% → 10% 15 CV, 10% 15 CV) to obtain **34** as slightly yellowish oil (326 mg, 0.71 mmol, 36 % yield).

R_f (*n*-heptane:EtOAc = 3:2) = 0.67 (CAM)

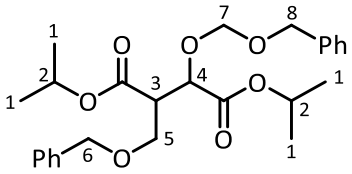

^{1}H NMR (400.27 MHz, $CDCl_3$, [42Oct0725/430]): δ_H: 7.26-7.42 (m, 10H, 2 × arom.), 5.05 (m, 2H, 2 × C**H** *i*Pr, 2), 4.83 (AB-system: A-part: d, J_{AB} = 7.2 Hz, B-part: d, J_{AB} = 7.2 Hz, 2H, 7), 4.63 (broad s, 2H, 8), 4.54 (d, J = 5.3 Hz, 4), 4.50 (ABX-system: A-part: dd, J_{AB} = 12.0 Hz, B-part: broad d, J_{AB} = 12.0 Hz, 6), 3.76 (ABX, A part: dd, J_{AB} = 9.5 Hz, J_{AX} = 6.5 Hz, B part: dd, J_{AB} = 9.5 Hz, J_{BX} = 7.5 Hz, 2H, 5), 3.27 (dt, J_{AX} = 6.5 Hz, J_{BX} = 7.5 Hz, 1H, 3), 1.57 (impurity: H_2O,), 1.12-1.35 (m, 12H, 4 × *i*Pr, 1) ppm.

4.3.4. Synthesis of diisopropyl 2-(benzyloxy)methyl-3-hydroxysuccinate (**73**)

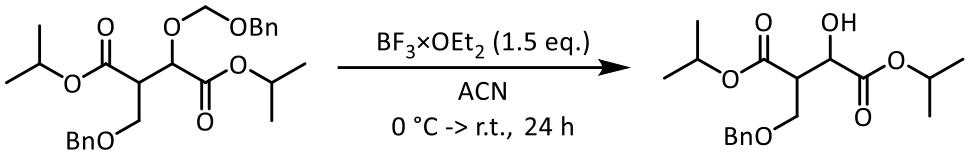

34 **73**

Boron trifluoride diethyl etherate (0.04 mL, 0.33 mmol, 1.5 eq.) was added to a stirred solution of **34** (0.1 g, 0.22 mmol, 1.0 eq.) in dry acetonitrile (2 mL) at 0 °C. After 24 hours, a saturated aqueous $NaHCO_3$ solution was added until neutral and the reaction mixture was extracted thrice with CH_2Cl_2. The combined organic phases were dried over Na_2SO_4 and the solvent was evaporated *in vacuo*. The product **73** (4 mg, 0.01 mmol, 5 % yield) was obtained as clear, colorless oil after purification by column chromatography (10 g silica, gradient of EtOAc in *n*-heptane: 2 % 1 CV, 2 → 20 % 12 CV).

R_f (*n*-heptane:EtOAc = 2:1) = 0.44 (CAM)

^{1}H NMR (400.27 MHz, $CDCl_3$, [41Oct1025/410]): δ_H: 7.33 (m, 5H, CH arom), 5.11 (sept, J = 6.3 Hz, 1H, *i*Pr), 5.02 (sept, J = 6.3 Hz, 1H, *i*Pr), 4.57 (AB-system: A-part: d, J = 11.6 Hz, B-part: d, J_{HH} = 11.6 Hz, 2H, C**H$_2$**), 4.49 (dd, J_{XH} = 2.7 Hz, $J_{X,OH}$ = 6.3 Hz, 1H, C**H**-OH), 3.85 (ABX-system: A-part: dd, J_{AB} = 9.3 Hz, J_{AX} = 6.0 Hz, B-part: dd, J_{AB} = 9.3 Hz, J_{BX} = 8.8 Hz, 2H, C**H$_2$**), 3.24 (d, $J_{X,OH}$ = 6.3 Hz, O**H**), 3.23 (ddd, J_{XH} = 2.7 Hz, J_{AX} = 6.0 Hz, J_{BX} = 8.8 Hz, 1H, C**H**-CH_2), 1.27 (dd, J = 4.2 Hz, J = 6.3 Hz, 6H, 2 × C**H$_3$**), 1.21 (d, J = 6.3 Hz, 6H, 2 × C**H$_3$**) ppm.

4.3.5. Synthesis of diisopropyl 2-(mesyloxy)succinate (**41**)

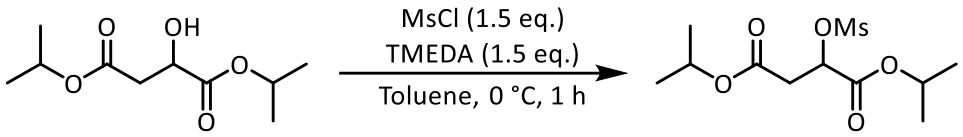

32 **41**

A solution of methane sulfonic chloride (0.45 mL, 349 mg, 1.5 eq.) in toluene (0.75 mL) was added to a stirred solution of malate **32** (437 mg, 2.0 mmol, 1.0 eq.) and tetramethyl ethylene diamine (0.34 mL, 344 mg, 3.0 mmol, 1.5 eq.) at 0 °C. After one hour of stirring at 0 °C, tetramethyl ethylene diamine (0.5 mL) was added, and the reaction mixture was extracted with ethyl acetate. The organic phases were combined, washed with H_2O, brine and dried over Na_2SO_4. After evaporation of the solvent under reduced pressure, the product was purified by column chromatography (25 g silica, gradient of EtOAc in *n*-heptane: 1 % 2 CV, 1 → 10 % 12 CV, 10 % 10 CV). **41** was obtained as clear oil (169 mg, 0.57 mmol, 29 % yield).

R_f (*n*-heptane:EtOAc = 2:1) = 0.57 (CAM)

^{1}H NMR (400.27 MHz, $CDCl_3$, [41Oct2125/170]): δ_H: 5.33 (dd, J_{AX} = 2.4 Hz, J_{BX} = 4.9 Hz, 1H, C**H**), 5.12 (sept, *J* = 6.3 Hz, 1H, 1 × *i*Pr), 5.05 (sept, *J* = 6.3 Hz, 1H, 1 × *i*Pr), 3.18 (s, 3H, C**H**$_3$ Ms), 2.92 (AB-system; A-part: d, J_{AB} = 4.9 Hz, J_{AX} = 2.4 Hz, B-part: dd, J_{AB} = 4.9 Hz, J_{BX} = 4.9 Hz 2H, C**H**$_2$),1.34-1.22 (m, 12H, 4 × C**H**$_3$ *i*Pr) ppm.

4.3.6. Synthesis of diisopropyl 2-(tosyloxy)succinate (**43**)

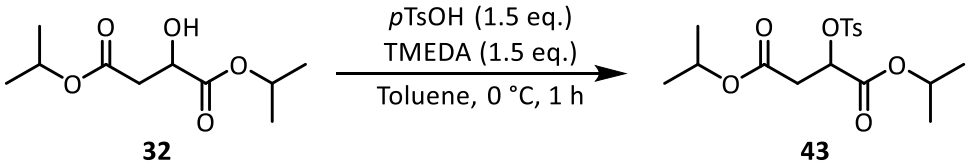

A solution of para-toluene sulfonic acid (572 mg, 3.0 mmol, 1.5 eq.) in toluene (0.75 mL) was added to a stirred solution of (±)-malate **32** (437 mg, 2.0 mmol, 1.0 eq.) and tetramethyl ethylene diamine (0.45 mL, 349 mg, 3.0 mmol, 1.5 eq.) at 0 °C. After one hour of constant stirring at 0 °C, water (1 mL) was added, and the mixture was extracted with ethyl acetate thrice. The organic phase was washed with H_2O and brine and then dried over Na_2SO_4. The solvent was evaporated under reduced pressure, and the product was purified by column chromatography (50 g silica, gradient of EtOAc in *n*-heptane: 2 % 2 CV, 2 → 15 % 20 CV, 15 % 6 CV) to obtain **43** as clear oil (300 mg, 0.81 mmol, 40 % yield).

R_f (*n*-heptane:EtOAc = 2:1) = 0.53 (UV)

^{1}H NMR (400.27 MHz, $CDCl_3$, [42Oct2125/400]): δ_H: 7.76 (d, *J* = 8.3 Hz, 2H, CH arom), 7.27 (d, *J* = 8.3 Hz, 2H, CH arom), 5.13 (dt, *J* = 1.0 Hz, *J* = 6.3 Hz, 1H, C**H**), 4.91 (sept, *J* = 6.3 Hz, 2 × 1H, 2 × *i*Pr), 2.79 (m, 2H, C**H**$_2$), 2.37 (s, 3H, C**H**$_3$ Ts), 1.24-1.06 (m, 12H, 4 × C**H**$_3$ *i*Pr) ppm.

4.3.7. Synthesis of ethyl glyoxylate (**47**)

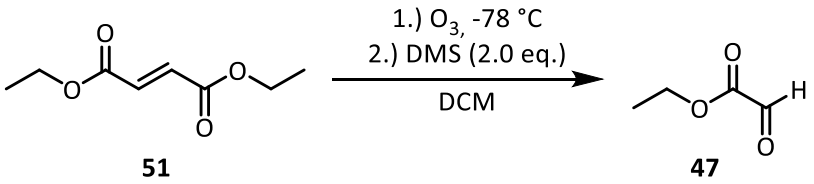

51 **47**

Dimethyl fumarate (**51**, 3.28 mL, 20.0 mmol, 1.0 eq.) was dissolved in 50 mL CH_2Cl_2 and ozone (flow: 80 L/h and 65 % O_3) was bubbled through the solution for 20 minutes at −78 °C. Dimethylsulfide (2.94 mL, 40.0 mmol, 2.0 eq.) was added and the reaction mixture was allowed to warm to room temperature. After solvent evaporation under reduced pressure, the mixture was purified by vacuum distillation (25 mm Hg, 48 °C) to obtain ethyl glyoxylate (**47**) as a clear, slightly yellowish oil (2.77 g, 27.1 mmol, 68 % yield).

^{1}H NMR (400.27 MHz, $CDCl_3$, [41Jan2226/1050]): δ_H: 9.40 (s, 1H, C(**H**)O), 4.39 (q, J_{HH} = 7.1 Hz, 2H, C**H**$_2$), 1.40 (t, J_{HH} = 7.1 Hz, 3H, C**H**$_3$) ppm.

4.3.8. Synthesis of ethyl 3-(diisopropoxyphosphoryl)-3-oxopropanoate (**46A** and its enolate **46B**)

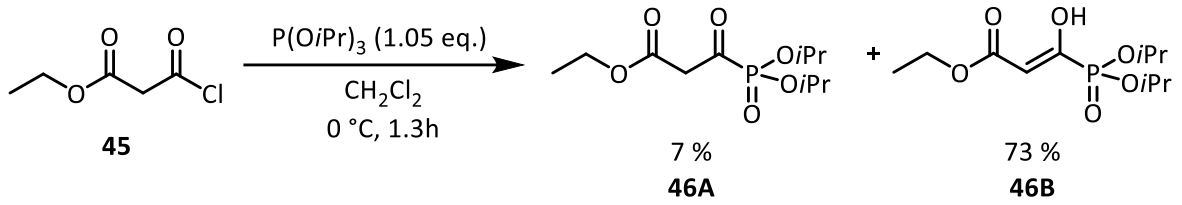

To a stirred solution of ethyl malonyl chloride (**45**, 3.84 mL, 30.0 mmol, 1.0 eq.) in CH_2Cl_2 (1.2 mL/mmol) triisopropyl phosphite (8.54 mL, 31.5 mmol, 1.05 eq.) was added slowly at 0 °C under argon. The reaction was followed by ^{31}P NMR and was stopped after 1.33 hours. All volatiles were removed under reduced pressure at room temperature. **46** was obtained as a mixture of its keto- (**46A**, 7 %) and enol (**46B**, 73 %) form as a slightly yellowish oil (10.24 g, purity: 80 mol%).

^{1}H NMR (400.27 MHz, $CDCl_3$, [42Feb1726/60]): δ_H: 11.65 (d, J_{HOP} = 29.1 Hz, 1H, O**H 46B**), 5.88 (d, J_{HP} = 10.0 Hz, 1H, enol-form C**H**), 4.77 (dsept, J_{HH} = 6.2 Hz, J_{HH} = 7.5 Hz, 2 × H, 2 × *i*Pr), 4.25 (q, J_{HH} = 7.1 Hz, 2H, C$\mathbf{H}_2$), 3.80 (unknown impurity), 3.34 (d, J_{PH} = 12.5 Hz, C$\mathbf{H}_2$ **46A**), 1.42-1.27 (m, 9H, 3 × C$\mathbf{H}_3$) ppm.

^{31}P NMR (162.03 MHz, $CDCl_3$, [42Feb1726/61]): δ_P: 4.45 (s, diisopropyl phosphite, ∫0.16), 3.14 (s, **46B**, ∫0.73), -3.33 (s, keto-form **46A**, ∫0.07), -5.84 (s, unknown impurity, ∫0.04) ppm.

4.3.9. Synthesis of (*R*)- and (*S*)-ethyl-3-(diisopropoxyphosphoryl)-3-hydroxy-propanoate [(*R*)- and (*S*)-**52**]

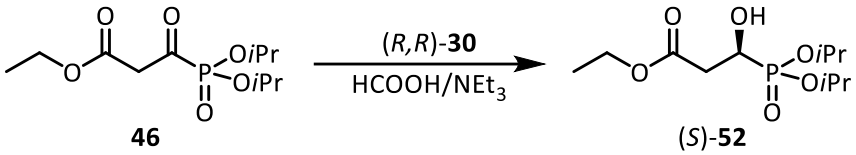

Compound (*S*)-**52** was synthesized according to general procedure **B**, followed by procedure **C** using compound **46** (2.64 g, 10.0 mmol, 1.0 eq.) as starting material and (*R,R*)-**30** (31.8 mg, 0.02 eq.) as catalyst. The reaction was stirred for 22 hours at 35 °C, before all volatiles were removed *in vacuo*. The crude was purified by column chromatography (10 g silica, gradient of EtOAc in *n*-heptane: 24 % → 100 % 3 CV, 100 % 8 CV) to obtain compound (*S*)-**52** (517 mg, 73 % yield) as yellowish oil.

R_f (100 % EtOAc) = 0.45 ($KMnO_4$)

^{1}H NMR (400.27 MHz, $CDCl_3$, [42Feb0926/600]): δ_H: 4.78 (sym. m, 2H, 2 × *i*Pr), 4.31 (m, 1H, C**H**), 4.20 (q, J_{HH} = 7.1 Hz, 2H, 2 × C**H$_2$** Et), 2.96 (dd, J_{HH} = 5.2 Hz, J_{HH} = 13.8 Hz, 1H, O**H**), 2.73 (ABXP-system; A-part: ddd, J_{AB} = 16.6 Hz, J_{AX} = 3.3 Hz, J_{AP} = 7.3 Hz, B-part: ddd, J_{AB} = 16.6 Hz J_{BX} = 7.9 Hz, J_{BP} = 10.1 Hz, 2H, 1 × C**H$_2$**), 1.35 (m, 12H, 4 × C**H$_3$** iPr), 1.28 (t, J_{HH} = 7.1 Hz, 3H, 1 × C**H$_3$** Et) ppm.

^{31}P NMR (162.03 MHz, $CDCl_3$, [42Feb0926/601]): δ_P: 20.67 ppm

(*R*)-**52** was synthesized similarly, starting from compound **46** (701 mg, 2.5 mmol, 1.0 eq.) but using (*S,S*)-**30** (30 mg, 0.019 eq.) as catalyst. The crude mixture was purified by column chromatography (10 g silica, gradient of EtOAc in *n*-heptane: 24 % EtOAc 1CV, 24 → 75 % 8CV, 75 % 13.7 CV) to obtain the product as a yellowish oil (660 mg, 94 % yield).

Spectroscopic data are identical to those of the other enantiomer.

A defined amount of compound either (*R*)- or (*S*)-**52** was weighed into an NMR tube together with 1.2 equivalents of the chiral solvating agent (*S*)-(-)-*tert*-butylphenylphosphinothioic acid [(*S*)-**53**], to determine the enantiomeric excess of these compouds.[53]

^{31}P NMR of (*R*)-**52** with chiral solvating agent [(*S*)-**53**] (162.03 MHz, $CDCl_3$, [41Feb0926/251]): δ_P: 93.99 (s, ∫3.52, chiral solvating agent), 22.07 [s, ∫1.00, complex of chiral solvating agent with (*R*)-**52**] ppm; *signal of complex of chiral solvating agent with (S)-**52** not detected;* ee ≥ 99.9 %.

^{31}P NMR of (*S*)-**52** with chiral solvating agent [(*S*)-**53**] (162.03 MHz, $CDCl_3$, [41Feb0926/241]): δ_P: 93.99 (s, ∫1.43, chiral solvating agent), 18.29 [s, ∫1.00, complex of chiral solvating agent with (*S*)-**52**] ppm; *signal of complex of chiral solvating agent with (R)-**52** not detected;* ee ≥ 99.9 %.

4.3.10. Synthesis of ethyl 2-((diisopropoxyphosphoryl)(hydroxy)methyl)-succinate (**58** or **59**)

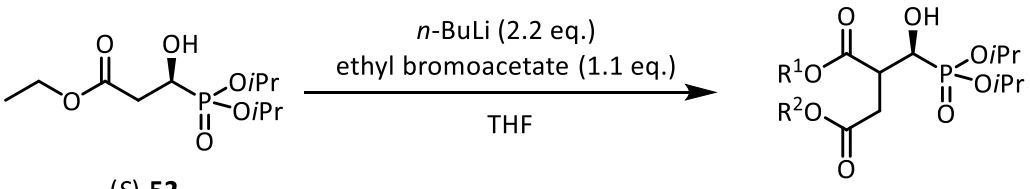

(*S*)-**52**

(*S*)-**58** or (*S*)-**59**

58, R^1 = Et, R^2 = H

59, R^1 = H, R^2 = Et

n-Butyl lithium (2.5 M, 1.76 mL, 4.4 mmol, 2.2 eq.) was added to a stirred solution of compound (*S*)-**52** (565 mg, 2.0 mmol, 1.0 eq.) in 2 mL dry THF at −50 °C under argon. After one hour, ethyl bromoacetate (0.24 mL, 2.2 mmol, 1.1 eq.) was added dropwise at −50 °C. After stirring for 4 hours between −40 and −50 °C, trifluoroacetic acid (0.35 mL) was added, followed by water and the phases were separated. The aqueous phase was washed thrice with ethyl acetate. The combined organic phases were washed with sat. aq. $NaHCO_3$ solution, brine and water and were dried with Na_2SO_4. Purification was performed by MPLC (25 g silica, gradient of EtOAc in *n*-heptane: 10 → 12 % 3.9 CV, 12 → 30 % 2 CV, 30 % 15 CV, 30 → 40 % 5 CV, 40 % 8.3 CV) to obtain **58** or **59** as a yellowish oil (63 mg, purity: 51 mol%).

Additional purification attempts to increase compound purity led to degradation hinting at acid lability of the compound.

R_f (*n*-heptane:EtOAc = 1:1) = 0.10 ($KMnO_4$)

R_f (100 % EtOAc) = 0.45 (CAM)

^{1}H NMR (400.27 MHz, $CDCl_3$, [41Mar1326/400]): only relevant peaks are given δ_H: 4.86-4.68 (sym. m, 2H, 2 × *i*Pr), 4.31 (dddd, J_{AX} = 3.4 Hz, J_{HX} = 13.0 Hz, J_{BX} = 8.1 Hz, J_{HP} = 5.4 Hz, 1H, C**H**), 4.19 (q, J_{HH} = 7.1 Hz, 2H, C**H$_2$** Et), 4.12 (q, J_{HH} = 7.1 Hz, 2H, C**H$_2$** Et), 3.81-3.70 (m, 1H, O**H**), 3.13 (dd, J_{HOH} = 3.4 Hz, J_{HX} = 13.0 Hz, C**H**-OH), 2.73 (ABXP-system; A-part: ddd, J_{AB} = 16.6 Hz, J_{AX} = 3.4 Hz, J_{AP} = 7.3 Hz, B-part: ddd, J_{AB} = 16.6 Hz J_{BX} = 8.1 Hz, J_{BP} = 10.1 Hz, 2H, 1 × C**H$_2$**), 1.35 (m, 12H, 4 × C**H$_3$** iPr), 1.28 (m, 3H, 1 × C**H$_3$** Et) ppm.

^{31}P NMR (162.03 MHz, $CDCl_3$, [41Mar1326/401]): δ_P: 57.6, 53.6, 39.9 (s, total ∫0.13, unknown impurity), 23.5 (s, ∫0.19, unknown impurity), 22.5 (s, ∫0.14, unknown impurity), 20.8 (s, ∫0.51, product) ppm.

4.3.11. Synthesis of triethyl ethene tricarboxylate (**62**)

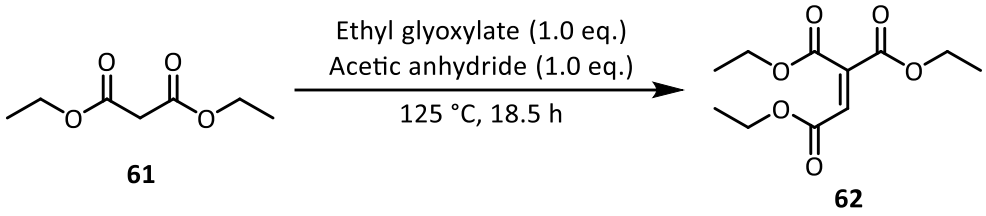

61 **62**

Diethyl malonate (**61**, 1.53 mL, 1.62 g, 10.0 mmol, 1.0 eq), ethyl glyoxalate (**47**, 0.99 mL, 1.02 g, 10.0 mmol, 1.0 eq.) and acetic anhydride (0.95 mL, 1.02 g, 10.0 mmol, 1.0 eq.) were mixed and stirred at 125 °C for 18.5 hours. Volatiles were removed by distillation at 60 °C (4 Torr). The residue was purified by MPLC (50 g silica, gradient of EtOAc in *n*-heptane: 6% → 40%) to yield **62** (924 mg, 38 % yield) as slightly yellowish oil.

R_f (*n*-heptane:EtOAc = 3:2) = 0.64 (UV)

^{1}H NMR (400.27 MHz, $CDCl_3$, [42Jan2626/210]): δ_H: 6.86 (s, 1H, C**H**), 4.37 (q, J_{HH} = 7.1 Hz, 2H, C**H**$_2$), 4.30 (q, J_{HH} = 7.1 Hz, 2H, C**H**$_2$), 4.25 (q, J_{HH} = 7.1 Hz, 2H, C**H**$_2$), 1.35 (t, J_{HH} = 7.1 Hz, 3H, C**H**$_3$), 1.32 (t, J_{HH} = 7.1 Hz, 3H, C**H**$_3$), 1.30 (t, J_{HH} = 7.1 Hz, 3H, C**H**$_3$) ppm.

4.3.12. Synthesis of diethyl formyl phosphonate (**68**)

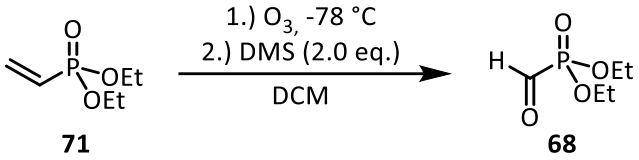

Diethyl vinyl phosphonate (**71**, 0.32 mL, 2.0 mmol, 1.0 eq.) was dissolved in 50 mL dry CH_2Cl_2 and ozone was bubbled through the solution for 15 minutes at −78 °C with an oxygen flow of 70 L/h and 65 % O_3. DMS (0.3 mL, 2.0 mmol, 2.0 eq.) was added at −78°C. The product **68** (purity: 39 mol%) was obtained in admixture with several unknown impurities and was used without further purification.

^{1}H NMR (400.27 MHz, $CDCl_3$, [41Mar1026/40]): only relevant signals are given δ_H: 8.29 (d, *J* = 11.7 Hz, -C(O)**H**), 4.06-4.19 (m, 4H, 2 × C**H**$_2$), 1.30-1.41 (m, 6H, 2 × C**H**$_3$) ppm.

^{31}P NMR (162.03 MHz, $CDCl_3$, [41Mar1026/41]): δ_P: 7.32 (s, ∫0.36, impurity: diethyl phosphite), 1.18 (s, ∫0.39, product), -2.77 (s, ∫0.05, unknown impurity), -5.26 (s, ∫0.07, unknown impurity), -8.38 (s, ∫0.13, unknown impurity) ppm.

5. Conclusion and Outlook

During this study, several strategies for the stereoselective synthesis of pantaphos and its saturated analogues were examined.

The initial synthetic approach commenced with malic acid as starting material and showed significant differences depending on the used malate esters (ethyl vs. isopropyl). A series of Fráter Seebach alkylations was performed with variations in temperature, reaction time, additive and solvent. Best results were achieved with shorter reaction times and ACN as additive for the addition of BOMCl as electrophile. Subsequent deprotection of the *O*-alkyl group was most effective with $BF_3 \times OEt_2$ as reagent, albeit only 17 % yield was achieved. Attempts to circumvent problems with the following deprotection step by using *O*-protected malate instead of malate were performed but led to equally low to no yields. Future experiments with LHMDS as base for the Fráter Seebach alkylation step are planned, instead of LDA.[46]

Other trials to obtain pantaphos using ethyl malonyl chloride as starting material were conducted. The latter was reacted with trialkyl phosphite to give a suitable precursor for further synthesis. Then, the intermediate was tested on varied base and electrophile combinations. Bases like LHMDS or *n*-BuLi performed best, albeit only at temperatures below −40 °C. In this context, ethyl bromoacetate was the only electrophile which was successfully added to the phosphonic acid analogue of malate. Still, only low yields were obtained for the α-hydroxy phosphonate **55**. Especially the purification of this compound will be subject of future investigations. This synthesis route shows potential to yield the desired product, but optimization of several steps such as the deprotonation of **46** and **52** with regard to temperature and reaction time are still needed.

Noteworthy, a successful asymmetric transfer hydrogenation of **46** using a Noyori-type catalyst can be reported. It was possible to determine the configuration and ee of the obtained enantiomers with high probability using a chiral solvating agent.[53]

First experiments using succinic and maleic anhydride as starting material were also conducted, unfortunately without success. This strategy will be evaluated in more detail in the future as maleic anhydride was shown to be a suitable reactant for various nucleophilic reactions.

Even though the synthesis of enantiopure pantaphos or its saturated analogues could not be achieved, this master's thesis evaluated several synthetic approaches to access the target compound. As such, valuable insight on the stability of various envisaged key intermediates was gained. This knowledge will be of great benefit for future studies on the stereoselective synthesis of (*R*)- and (*S*)-pantaphos.

6. References

(1) Rodriguez, J. B.; Gallo-Rodriguez, C. The Role of the Phosphorus Atom in Drug Design. *ChemMedChem* **2019**, *14* (2), 190–216. https://doi.org/10.1002/cmdc.201800693.

(2) McGrath, J. W.; Chin, J. P.; Quinn, J. P. Organophosphonates Revealed: New Insights into the Microbial Metabolism of Ancient Molecules. *Nat. Rev. Microbiol.* **2013**, *11* (6), 412–419. https://doi.org/10.1038/nrmicro3011.

(3) Metcalf, W. W.; Van Der Donk, W. A. Biosynthesis of Phosphonic and Phosphinic Acid Natural Products. *Annu. Rev. Biochem.* **2009**, *78* (1), 65–94. https://doi.org/10.1146/annurev.biochem.78.091707.100215.

(4) Krečmerová, M.; Majer, P.; Rais, R.; Slusher, B. S. Phosphonates and Phosphonate Prodrugs in Medicinal Chemistry: Past Successes and Future Prospects. *Front. Chem.* **2022**, *10*, 889737. https://doi.org/10.3389/fchem.2022.889737.

(5) Dinhof, T. Synthesis of Organophosphorus Compounds for Use in Chemical Biology Research. https://doi.org/10.25365/thesis.75928.

(6) Crumpacker, C. S. Mechanism of Action of Foscarnet against Viral Polymerases. *Am. J. Med.* **1992**, *92* (2), S3–S7. https://doi.org/10.1016/0002-9343(92)90329-A.

(7) Gérard, L.; Salmon-Céron, D. Pharmacology and Clinical Use of Foscarnet. *Int J Antimicrob Agents*. https://doi.org/https://doi.org/10.1016/0924-8579(95)00008-v.

(8) Wang, L.; Fang, D.; Xu, J.; Luo, R. Various Pathways of Zoledronic Acid against Osteoclasts and Bone Cancer Metastasis: A Brief Review. *BMC Cancer* **2020**, *20* (1), 1059. https://doi.org/10.1186/s12885-020-07568-9.

(9) Budzinska, A.; Jarmuszkiewicz, W. The Cellular and Mitochondrial Consequences of Mevalonate Pathway Inhibition by Nitrogen-Containing Bisphosphonates: A Narrative Review. *Pharmaceuticals* **2025**, *18* (7), 1029. https://doi.org/10.3390/ph18071029.

(10) Silver, L. L. Fosfomycin: Mechanism and Resistance. *Cold Spring Harb. Perspect. Med.* **2017**, *7* (2), a025262. https://doi.org/10.1101/cshperspect.a025262.

(11) Zhu, J.-Y.; Yang, Y.; Han, H.; Betzi, S.; Olesen, S. H.; Marsilio, F.; Schönbrunn, E. Functional Consequence of Covalent Reaction of Phosphoenolpyruvate with UDP-N-Acetylglucosamine 1-Carboxyvinyltransferase (MurA). *J. Biol. Chem.* **2012**, *287* (16), 12657–12667. https://doi.org/10.1074/jbc.M112.342725.

(12) Pallitsch, K. „Studies on the Biodegradation of P-C Compounds – Phosphonic Acids as Enzyme Inhibitors“.

(13) Zhou, H.; Meng, L.; Yin, X.; Liu, Y.; Wu, J.; Xu, G.; Wu, M.; Yang, L. Biocatalytic Asymmetric Synthesis of L-Phosphinothricin Using a One-Pot Three Enzyme System and a Continuous Substrate Fed-Batch Strategy. *Appl. Catal. Gen.* **2020**, *589*, 117239. https://doi.org/10.1016/j.apcata.2019.117239.

(14) Mowbray, S.; Kathiravan, M.; Pandey, A.; Odell, L. Inhibition of Glutamine Synthetase: A Potential Drug Target in Mycobacterium Tuberculosis. *Molecules* **2014**, *19* (9), 13161–13176. https://doi.org/10.3390/molecules190913161.

(15) Wild, A.; Manderscheid, R. The Effect of Phosphinothricin on the Assimilation of Ammonia in Plants. *Z. Für Naturforschung C* **1984**, *39* (5), 500–504. https://doi.org/10.1515/znc-1984-0539.

(16) Qu, R.; He, B.; Yang, J.; Lin, H.; Yang, W.; Wu, Q.; Li, Q. X.; Yang, G. Where Are the New Herbicides? *Pest Manag. Sci.* **2021**, *77* (6), 2620–2625. https://doi.org/10.1002/ps.6285.

(17) Baćmaga, M.; Wyszkowska, J.; Kucharski, J. Environmental Implication of Herbicide Use. *Molecules* **2024**, *29* (24), 5965. https://doi.org/10.3390/molecules29245965.

(18) Gianessi, L. P. The Increasing Importance of Herbicides in Worldwide Crop Production. *Pest Manag. Sci.* **2013**, *69* (10), 1099–1105. https://doi.org/10.1002/ps.3598.
(19) Kumar, K.; Gambhir, G.; Dass, A.; Tripathi, A. K.; Singh, A.; Jha, A. K.; Yadava, P.; Choudhary, M.; Rakshit, S. Genetically Modified Crops: Current Status and Future Prospects. *Planta* **2020**, *251* (4), 91. https://doi.org/10.1007/s00425-020-03372-8.
(20) Kudsk, P. Optimising Herbicide Dose: A Straightforward Approach to Reduce the Risk of Side Effects of Herbicides. *The Environmentalist* **2008**, *28* (1), 49–55. https://doi.org/10.1007/s10669-007-9041-8.
(21) Monçon Fipke, G.; Martin, T. N.; Nunes, U. R.; Deak, V. A.; Leivas Stecca, J. D.; Minussi Winck, J. E.; Teleken Grando, L. F.; Da Costa Rossato, A. Application of Non-Selective Herbicides in the Pre-Harvest of Wheat Damages Seed Quality. *Am. J. Plant Sci.* **2018**, *09* (01), 107–123. https://doi.org/10.4236/ajps.2018.91010.
(22) Shimabukuro, R. H.; Swanson, H. R. Atrazine Metabolism, Selectivity, and Mode of Action. *J. Agric. Food Chem.* **1969**, *17* (2), 199–205. https://doi.org/10.1021/jf60162a044.
(23) Evans, A. F.; O'Brien, S. R.; Ma, R.; Hager, A. G.; Riggins, C. W.; Lambert, K. N.; Riechers, D. E. Biochemical Characterization of Metabolism-based Atrazine Resistance in *Amaranthus Tuberculatus* and Identification of an Expressed *GST* Associated with Resistance. *Plant Biotechnol. J.* **2017**, *15* (10), 1238–1249. https://doi.org/10.1111/pbi.12711.
(24) Islam, F.; Wang, J.; Farooq, M. A.; Khan, M. S. S.; Xu, L.; Zhu, J.; Zhao, M.; Muños, S.; Li, Q. X.; Zhou, W. Potential Impact of the Herbicide 2,4-Dichlorophenoxyacetic Acid on Human and Ecosystems. *Environ. Int.* **2018**, *111*, 332–351. https://doi.org/10.1016/j.envint.2017.10.020.
(25) Aoun, P. G.; Khairallah, W.; Rejeb, A.; Haddarah, A. Glyphosate Use in Crop Systems: Risks to Health and Sustainable Alternatives. *Toxics* **2025**, *13* (11), 971. https://doi.org/10.3390/toxics13110971.
(26) Benbrook, C. M. Trends in Glyphosate Herbicide Use in the United States and Globally. *Environ. Sci. Eur.* **2016**, *28* (1), 3. https://doi.org/10.1186/s12302-016-0070-0.
(27) Bhatt, P.; Joshi, T.; Bhatt, K.; Zhang, W.; Huang, Y.; Chen, S. Binding Interaction of Glyphosate with Glyphosate Oxidoreductase and C–P Lyase: Molecular Docking and Molecular Dynamics Simulation Studies. *J. Hazard. Mater.* **2021**, *409*, 124927. https://doi.org/10.1016/j.jhazmat.2020.124927.
(28) Van Bruggen, A. H. C.; He, M. M.; Shin, K.; Mai, V.; Jeong, K. C.; Finckh, M. R.; Morris, J. G. Environmental and Health Effects of the Herbicide Glyphosate. *Sci. Total Environ.* **2018**, *616–617*, 255–268. https://doi.org/10.1016/j.scitotenv.2017.10.309.
(29) Herrmann, K. M. The Shikimate Pathway: Early Steps in the Biosynthesis of Aromatic Compounds.
(30) Sammons, R. D.; Gruys, K. J.; Anderson, K. S.; Johnson, K. A.; Sikorski, J. A. Reevaluating Glyphosate as a Transition-State Inhibitor of EPSP Synthase: Identification of an EPSP Synthase.Cntdot.EPSP.Cntdot.Glyphosate Ternary Complex. *Biochemistry* **1995**, *34* (19), 6433–6440. https://doi.org/10.1021/bi00019a024.
(31) Marzabadi, M. R.; Gruys, K. J.; Pansegrau, P. D.; Walker, M. C.; Yuen, H. K.; Sikorski, J. A. An EPSP Synthase Inhibitor Joining Shikimate 3-Phosphate with Glyphosate: Synthesis and Ligand Binding Studies. *Biochemistry* **1996**, *35* (13), 4199–4210. https://doi.org/10.1021/bi9521349.
(32) Sviridov, A. V.; Shushkova, T. V.; Ermakova, I. T.; Ivanova, E. V.; Epiktetov, D. O.; Leontievsky, A. A. Microbial Degradation of Glyphosate Herbicides (Review). *Appl.*

Biochem. Microbiol. **2015**, *51* (2), 188–195. https://doi.org/10.1134/S0003683815020209.
(33) Ruffolo, F.; Dinhof, T.; Murray, L.; Zangelmi, E.; Chin, J. P.; Pallitsch, K.; Peracchi, A. The Microbial Degradation of Natural and Anthropogenic Phosphonates. *Molecules* **2023**, *28* (19), 6863. https://doi.org/10.3390/molecules28196863.
(34) Brock, A. L.; Rein, A.; Polesel, F.; Nowak, K. M.; Kästner, M.; Trapp, S. Microbial Turnover of Glyphosate to Biomass: Utilization as Nutrient Source and Formation of AMPA and Biogenic NER in an OECD 308 Test. *Environ. Sci. Technol.* **2019**, *53* (10), 5838–5847. https://doi.org/10.1021/acs.est.9b01259.
(35) Fortes, C.; Mastroeni, S.; Segatto, M. M.; Hohmann, C.; Miligi, L.; Bakos, L.; Bonamigo, R. Occupational Exposure to Pesticides With Occupational Sun Exposure Increases the Risk for Cutaneous Melanoma. *J. Occup. Environ. Med.* **2016**, *58* (4), 370–375. https://doi.org/10.1097/JOM.0000000000000665.
(36) Krüger, M.; Schrödl, W.; Pedersen, I. Detection of Glyphosate in Malformed Piglets. *J. Environ. Anal. Toxicol.* **2014**, *04* (05). https://doi.org/10.4172/2161-0525.1000230.
(37) Camacho, A.; Mejía, D. The Health Consequences of Aerial Spraying Illicit Crops: The Case of Colombia. *J. Health Econ.* **2017**, *54*, 147–160. https://doi.org/10.1016/j.jhealeco.2017.04.005.
(38) Polidore, A. L. A.; Caserio, A. D.; Zhu, L.; Metcalf, W. W. Complete Biochemical Characterization of Pantaphos Biosynthesis Highlights an Unusual Role for a SAM-Dependent Methyltransferase. *Angew. Chem. Int. Ed.* **2024**, *63* (7), e202317262. https://doi.org/10.1002/anie.202317262.
(39) Polidore, A. L. A.; Furiassi, L.; Hergenrother, P. J.; Metcalf, W. W. A Phosphonate Natural Product Made by Pantoea Ananatis Is Necessary and Sufficient for the Hallmark Lesions of Onion Center Rot. *mBio* **2021**, *12* (1), e03402-20. https://doi.org/10.1128/mBio.03402-20.
(40) Guin, J.; Wang, Q.; van Gemmeren, M.; List, B. The Catalytic Asymmetric Abramov Reaction. *Angew. Chem. Int. Ed.* **2015**, *54* (1), 355–358. https://doi.org/10.1002/anie.201409411.
(41) Henning, H.; Hilgetag, G. Möglichkeiten und Grenzen der Michaelis-Arbusow-Reaktion. *Z. Für Chem.* **1967**, *7* (5), 169–176. https://doi.org/10.1002/zfch.19670070502.
(42) Sun, Z.; Xiao, L.; Chen, Y.; Wang, J.; Zeng, F.; Zhang, H.; Zhang, J.; Yang, K.; Hu, Y. J. Constructive On-DNA Abramov Reaction and Pudovik Reaction for DEL Synthesis. *ACS Med. Chem. Lett.* **2023**, *14* (4), 473–478. https://doi.org/10.1021/acsmedchemlett.3c00022.
(43) Rádai, Z.; Keglevich, G. Synthesis and Reactions of α-Hydroxyphosphonates. *Molecules* **2018**, *23* (6), 1493. https://doi.org/10.3390/molecules23061493.
(44) Noyori, R. Asymmetric Catalysis: Science and Opportunities (Nobel Lecture). *Angew. Chem. Int. Ed.* **2002**, *41* (12), 2008–2022. https://doi.org/10.1002/1521-3773(20020617)41:12%3C2008::AID-ANIE2008%3E3.0.CO;2-4.
(45) Polidore, A. L. A.; Furiassi, L.; Hergenrother, P. J.; Metcalf, W. W. A Phosphonate Natural Product Made by Pantoea Ananatis Is Necessary and Sufficient for the Hallmark Lesions of Onion Center Rot. *mBio* **2021**, *12* (1), e03402-20. https://doi.org/10.1128/mBio.03402-20.
(46) Xue, F.; Gu, W.; Silverman, R. B. Concise Route to the Chiral Pyrrolidine Core of Selective Inhibitors of Neuronal Nitric Oxide. *Org. Lett.* **2009**, *11* (22), 5194–5197. https://doi.org/10.1021/ol902109t.

(47) Frater, G.; Günther, W.; Müller, U. The Stereoselective Alpha-Alkylation of Chiral Beta-Hydroxy Esters and Some Applications Thereof.
(48) Ueki, T.; Kinoshita, T. Stereoselective Synthesis and Structure of Butalactin and Lactone II Isolated from Streptomyces Species. *Org. Biomol. Chem.* **2004**, *2* (19), 2777. https://doi.org/10.1039/b407820a.
(49) Yoshida, Y. Facile and Practical Methods for the Sulfonylation of Alcohols Using Ts(Ms)Cl and Me2N(CH2)nNMe2 as a Key Base. *Synthesis* **1999**, *1999* (09), 1633–1636. https://doi.org/10.1055/s-1999-3561.
(50) Scheibelberger, L.; Stankovic, T.; Liepert, K.; Kienzle, A.; Patronas, E.; Balber, T.; Mitterhauser, M.; Haschemi, A.; Pallitsch, K. Fluorinated Analogues to the Pentuloses of the Pentose Phosphate Pathway. *Eur. J. Org. Chem.* **2023**, *26* (31), e202300339. https://doi.org/10.1002/ejoc.202300339.
(51) Cabezon, B.; Cao, J.; Raymo, F. M.; Stoddart, J. F.; White, A. J. P.; Williams, D. J. Self-Complementary Catenanes and Their Related Catenanes. *Chem. - Eur. J.* **2000**, *6* (12), 2262–2273. https://doi.org/10.1002/1521-3765(20000616)6:12%253C2262::AID-CHEM2262%253E3.0.CO;2-G.
(52) Dinhof, T.; Kalina, T.; Stanković, T.; Braunsteiner, K.; Rohrbach, P.; Turhan, E.; Gradwohl, A.; Königshofer, A.; Horak, J.; Pallitsch, K. Asymmetric Transfer Hydrogenation as a Key Step in the Synthesis of the Phosphonic Acid Analogs of Aminocarboxylic Acids. *Chem. – Eur. J.* **2023**, *29* (72), e202302171. https://doi.org/10.1002/chem.202302171.
(53) Drescher, M.; Felsinger, S.; Hammerschmidt, F.; Kählig, H.; Schmidt, S.; Wuggenig, F. EVALUATION OF HOMOCHIRAL T-BUTYL(PHENYL)PHOSPHINOTHIOIC ACID FOR THE DETERMINATION OF ENANTIOMERIC EXCESSES AND ABSOLUTE CONFIGURATIONS OF α-SUBSTITUTED PHOSPHONATES. *Phosphorus Sulfur Silicon Relat. Elem.* **1998**, *140* (1), 79–93. https://doi.org/10.1080/10426509808035734.
(54) Evans, S. B.; Abdelkader, M.; Padias, A. B.; Hall, H. K. Synthesis and Reactions of A-Carbomethoxy-N-Phenylmaleimideand Related Electrophilic Ethylenes.
(55) Mohamed, S. A.; Debello, M.; Cantot, J.; Lavaud, S.; Chollet, G.; Queffélec, C.; Chailleux, E. The Reaction of Maleic Anhydride with Alkenes: A Review on the Mechanisms Involved in the Reaction of Maleic Anhydride with Lipids. *Green Chem.* **2025**, *27* (28), 8386–8413. https://doi.org/10.1039/D5GC00543D.
(56) Stauffer, F.; Neier, R. Synthesis of Tri- and Tetrasubstituted Furans Catalyzed by Trifluoroacetic Acid. *Org. Lett.* **2000**, *2* (23), 3535–3537. https://doi.org/10.1021/ol0063205.
(57) Morgalyuk, V. Chemistry of Phosphorylated Formaldehyde Derivatives. Part I. *Molecules* **2014**, *19* (9), 12949–13009. https://doi.org/10.3390/molecules190912949.
(58) *Handbook of Maleic Anhydride Based Materials*; Musa, O. M., Ed.; Springer International Publishing: Cham, 2016. https://doi.org/10.1007/978-3-319-29454-4.